Investigation of hydrostratigraphic units of the Santa Fe Group aquifer in the northwestern Albuquerque Basin, New Mexico

Daniel Koning*, Luke Martin, Matthew Zimmerer, Ethan Mamer, Amanda Doherty, and Laila Sturgis

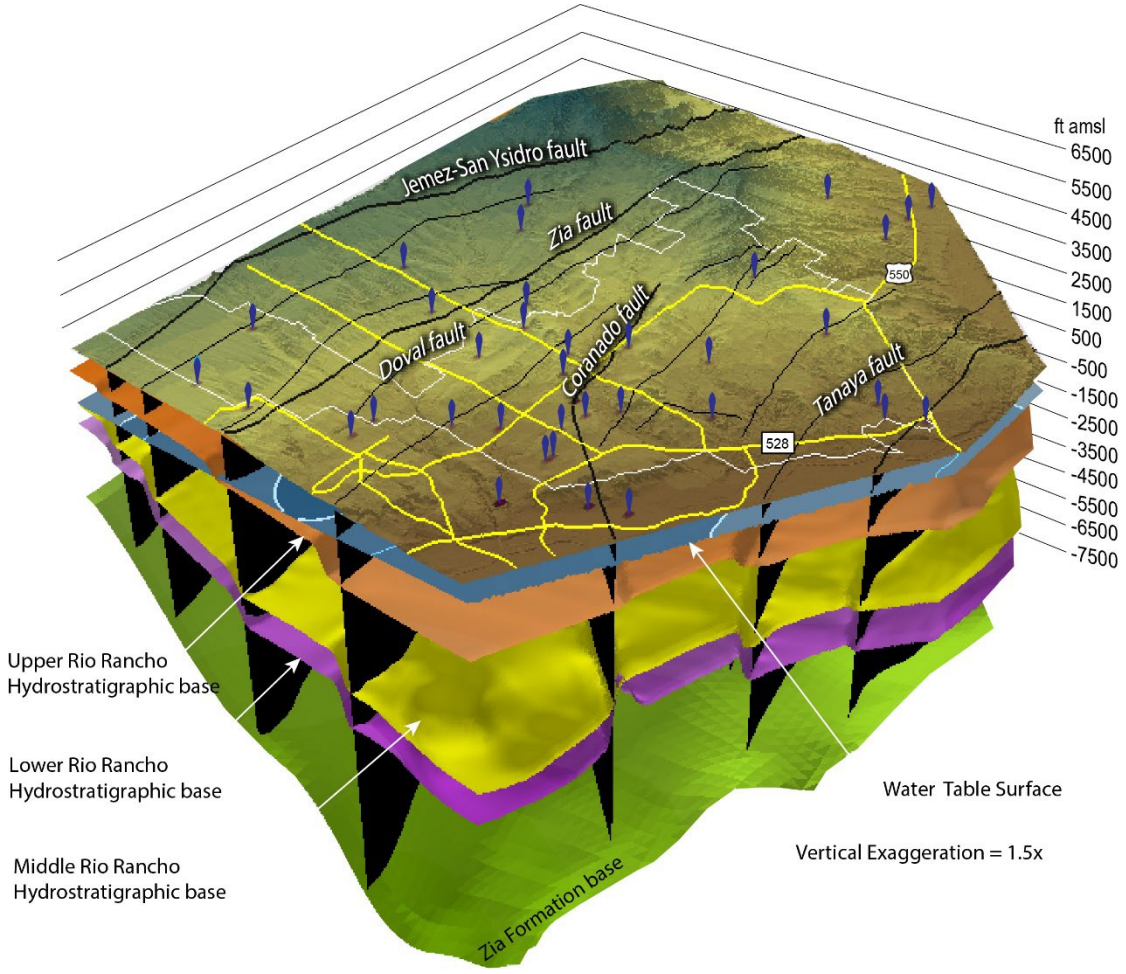

OFR XXXX

January, 2025

New Mexico Bureau of Geology and Mineral Resources, New Mexico Institute of Mining and Technology

801 Leroy Place, Socorro, NM 87801

* Email: dan.koning@nmt.edu

EXECUTIVE SUMMARY

The purposes of this study are to delineate and map (in the subsurface) hydrostratigraphic units (HSU) within the Santa Fe Group aquifer found in the northwest part of the Albuquerque basin, and to assess the permeability differences between and within those units. A hydrostratigraphic unit is a zone in an aquifer that has unique physical properties pertaining to groundwater, such as permeability, porosity, yield, or hydraulic conductivity. In our study, four HSUs, corresponding to stratigraphic layers typically hundreds to thousands of feet thick (>100 m thick), could be correlated across the study area using downhole geophysical (wireline) data in 30 wells (particularly resistivity, neutron, and gamma-ray data). These HSUs (and their lithostratigraphic counterparts per Connell, 2008a) are: Upper Rio Rancho HSU (Ceja Formation, Picuda Peak Member of the Arroyo Ojito Formation); Middle Rio Rancho HSU (Loma Barbon and Navajo Draw Members of the Arroyo Ojito Formation and the Benavidez member of Koning et al., 2021); Lower Rio Rancho HSU (upper, sand-dominated part of the Cerro Conejo Formation); and the Zia HSU (middle-lower Cerro Conejo Formation plus all of the Zia Formation, extending down to bedrock).

Three-dimensional mapping of the Santa Fe Group aquifer entailed constructing stacked raster surfaces corresponding to the bounding surfaces of the HSUs. Contours of each of the HSU surfaces were drawn manually in ArcMap GIS software. We began contouring a given HSU surface where it was exposed in escarpments near La Ceja and Ceja del Rio Puerco, and extrapolated the contact into the subsurface (south and eastward) using available map attitude data and HSU-elevation picks in the aforementioned 30 wells. Major faults were explicitly incorporated into the 3D mapping, and HSU contacts were offset by fault lines using displacements inferred from cross sections or from geologic mapping. This procedure was employed for the tops of the Zia HSU, Lower Rio Rancho HSU, and the Middle Rio Rancho HSU. The top of the Upper Rio Rancho HSU corresponds to surface topography. We used a raster of the top-of-bedrock (constructed by Grauch and Connell, 2013, given to us by V.J.S. Grauch) for the base of the Zia HSU. The contours and the elevations of the HSU contacts at the 30 wells were used as inputs in the Topo to Raster ArcGIS tool, whose output for each contact is a raster image with 50 m grid spacing.

To determine the extent and volume of saturated zones within each HSU, the approximate potentiometric surface was mapped using groundwater-level measurements from 58 wells across the study area, where water levels were measured from 1985-2021 with most data collected during 2008-

2021. In order to cover the entire study area, seven water level measurements were included near the northern and western boundaries of the study area that date between 1956 through 1984. The groundwater elevation data from these wells were contoured in ArcMap and then converted to a raster image using the Topo to Raster ArcGIS tool.

The saturated tops and bases of each HSU needed to be determined in order to map saturated thicknesses in each HSU. To calculate the saturated thickness of a given HSU, the saturated base of that HSU was subtracted from the saturated top of the HSU or, where the top was not saturated, the sloping potentiometric surface within the HSU.

We produced elevation-contour maps for the tops of the HSUs and the tops of the saturated zone within a HSU. In addition, we provide a 3D visualization of the Santa Fe Group by stacking the HSU raster surfaces and incorporating the potentiometric surface in this visualization. These products and the detailed investigation of well logs support the following interpretations: 1) HSUs and saturated HSUs thicken eastward across the Zia and San Ysidro faults. 2) East of the Zia fault, both HSUs and saturated HSUs thicken southward and southeastward, becoming thickest in the southeast corner of the study area (near the intersection of Paseo del Norte and Coors). 3) Relatively thickened HSUs, most notably the Middle Rio Rancho HSU, extend northwards in the Montoyas graben (new name; structure approximately coincides with the upper reaches of Arroyo de los Montoyas) that is bounded on the west by the Zia fault and the east by the Coronado-Alamdeda fault and Ziana horst. 4) The Upper and Middle HSUs (and saturated HSUs) become thinner eastward across a geologic structure called the Ziana horst, and pinch-out northwards on this structure. 5) To the east of the Tamaya fault, the Upper and Middle Rio Rancho HSUs thicken under the city of Bernalillo. 6) The Middle Rio Rancho HSU commonly displays a coarsening-upward trend. 7) The apparent lack of notable thinning of the Lower Rio Rancho HSU across the Ziana horst, coupled with 500–1,000 ft of apparent vertical displacement of a 11.2-11.3 Ma ash zone by a fault bounding the eastern side of the horst, indicate notable tectonic activity associated with the horst after 11 Ma. In addition, thinning of the Upper and Middle Rio Rancho HSUs across the Ziana horst and thickening in the Montoyas graben indicates late Miocene tectonic-controlled stratal thickening.

Permeability assessments were conducted using three methods. The first method entailed outcrop mapping of the two HSUs that made vertical faces: the upper Zia HSU (i.e., middle-lower Cerro Conejo Formation) and the Middle Rio Rancho HSU (Arroyo Ojito Formation). The outcrop mapping was conducted on base imagery consisting of stitched, high-resolution photographs taken by unmanned

aerial vehicles. Two outcrops of the upper Zia HSU and four outcrops of the Middle Rio Rancho HSU were analyzed. Contacts separating sand vs clayey sediment (clayey sand or clay-silt beds) were delineated on this imagery using ArcMap GIS software, and various ArcGIS tools were used to calculate the 2D proportion of the following permeability proxies: sand vs clayey sand in a given image, sand body thicknesses, and the amalgamation ratio (length of sand-on-sand contacts vs. total contact lengths). These analyses suggest slightly more favorable permeability proxies in the upper Zia HSU compared to the Middle Rio Rancho HSU. We infer that the relatively restricted spatial extent of this method, particularly in terms of the proportion of the studied stratigraphic interval relative to the thickness of the entire unit, imparts higher uncertainty in this approach, especially vertical trends, compared to various permeability-related data in wells.

The second permeability assessment consisted of detailed differentiation of sand vs. clayey sediment in 22 wells (interpreted from wireline logs with the aid of cuttings) for stratigraphic intervals in the saturated part of HSUs. The resulting data indicate the highest non-clayey sediment (i.e., clean sand) ratios are in the Upper Rio Rancho HSU and the Lower Rio Rancho HSU. Assuming clay-poor sediment is a proxy for higher permeability, this analysis suggests higher permeability for the Upper and Lower Rio Rancho HSUs.

The third permeability assessment involved compilation of hydraulic conductivity values from pumping tests for wells that were screened in greater-than 80% of either the Upper, Middle or Lower Rio Rancho HSUs. Pumping test data were lacking for the Zia HSU. We plotted these hydraulic conductivity (K) values per HSU on a box and whisker plot to compare differences between HSUs. We also plotted the K values on a map to visually compare any spatial trends within a HSU. These analyses indicate that the Upper Rio Rancho HSU exhibits higher K values and is the more permeable HSU compared to the Middle Rio Rancho HSU, consistent with its higher sand proportions (at a given location) and higher density-porosity values in its sand bodies (the latter probably reflecting less compaction and less cementation). Based on a single pumping test (Rio Rancho Utility Well 23), the Lower Rio Rancho HSU may also have relatively high hydraulic conductivity, consistent with the second permeability assessment results, but more pumping-test data are needed to confirm that possibility. No lateral trends were apparent in the Upper Rio Rancho HSU. In the Middle Rio Rancho HSU, pumping-test data suggest higher hydraulic conductivity values in the southwest part of the study area, west of the west end of Paseo del Norte. We speculate that these higher conductivity values may be reflective of coarse sand tongues associated with the Benavidez member of Koning et al. (2021), which is a sandy

Santa Fe Group lithostratigraphic unit derived from erosion of a thick, gravelly sand layer that once capped the southeastern Colorado Plateau. North of approximately 35° 20'00" north latitude, there may possibly be a northward lateral trend in the Middle Rio Rancho HSU to increased sand concentrations and higher permeabilities, but more data is needed to confirm this increase.

To better understand groundwater quality and recharge, we compiled from preexisting studies (Plummer et al., 2004a,b,c) radiocarbon ages and total dissolved solids (TDS) measurements per well. Wells with elevated TDS are spatially associated with the Ziana horst and possibly the Lower Rio Rancho HSU, suggesting the possibility that faults bounding the horst may be expelling salty groundwater from fractured, structurally elevated bedrock; similar expelling may adversely affect the Lower Rancho and Zia HSUs across the study area. Radiocarbon ages are oldest in the northwest part of the study area (in the Middle Rio Grande HSU) and youngest in the southeast corner of the study area near the Rio Grande (in the Upper Rio Grande HSU). Given the westward slope of the potentiometric-elevation surface in the southeast corner of the study area, these data suggest a component of recharge to the Upper Rio Grande HSU from the Rio Grande. In contrast, the >20,000 year radiocarbon ages in the northwestern study area, west of the Zia fault and near Rio Rancho Utility Well 9, suggest minimal recharge there.

Collectively, our study's data HSU mapping provides guidance regarding groundwater management for the Santa Fe Group aquifer in the Rio Rancho area. Building on the hydrochemical zones of Plummer et al. (2020a,c), we propose five hydrogeologic regimes based on groundwater chemistry, inferred groundwater flow direction, and faults that appear to impact groundwater flow. Even though the groundwater is of relatively good quality in the Middle Rio Rancho HSU in the west and northwest part of the study area (in the northern West-central regime), it is a limited quantity and several hundred feet below ground surface; in addition, old radiocarbon ages and notable cones of depression suggest relatively low permeabilities and limited recharge to that area. The higher TDS values found near the Ziana horst (Ziana regime) is a deterrent for future well drilling there unless economic blending with fresher water can be achieved. East of the Ziana horst and in the southern part of the study area, east of approximately Universe Boulevard (central regime), coincides with the thickest saturated HSUs, including the high-permeability Upper Rio Rancho HSU, and exhibits relatively low TDS and young radiocarbon ages. These areas are interpreted to be the most favorable for groundwater extraction. Our 3D hydrostratigraphic model and compiled hydraulic conductivities can be used in future studies pertaining to groundwater flow and management in the northwestern Albuquerque Basin.

INTRODUCTION

Purpose

The purpose of this study is to delineate hydrostratigraphic units (HSU) in the Santa Fe Group of the northwestern Albuquerque Basin and map these units in the subsurface. We also assess permeability differences between HSUs and laterally within a given HSU using pump-test hydraulic conductivities and permeability proxies; these proxies include sediment texture (i.e., proportion of clay), sand body thickness, and sand body amalgamation ratios. As ancillary products, the following were constructed: an approximate groundwater-elevation (potentiometric surface) map and depth-to-groundwater map, a map of compiled TDS values (per well and per HSU), and a map of compiled radiocarbon ages (per well and per HSU). The study was initiated and paid for by the City of Rio Rancho so they may more effectively plan future well sites and manage groundwater resources.

Study Area

The study area is located in the northwestern part of the Albuquerque basin, ~30-45 mi (~50-70 km) northwest of downtown Albuquerque (Fig. 1). It is underlain by variable thicknesses of the Santa Fe Group, which is comprised of sand-dominated, clastic sediment intercalated with minor volcanic rocks; the Santa Fe Group aggraded in the Rio Grande rift while it was subsiding during the late Oligocene through early Pleistocene (Spiegel and Baldwin, 1963; Chapin and Cather, 1994). The study area includes the City of Rio Rancho and extends several kilometers northward and westward from the municipality's northern and western boundaries, respectively (Fig. 2). The placement of the western and northern boundaries allows mapped outcrops of exposed HSUs to be incorporated into the 3D map of these units. Important wells used in our study and major faults are plotted on the study area map of Figure 2.

Much of the study area is underlain by the mesa-like feature called Llano de Albuquerque (Fig. 1). The west and north sides of the "Llano" correspond to steep slopes and badlands called the La Ceja del Rio Puerco and La Ceja (Fig. 1). This badland topography grades westward and northward, respectively, into the broad valley floors of the Rio Puerco and Jemez River. The Llano del Albuquerque slopes eastward towards the Rio Grande, which is along the eastern border of the study area.

Previous work

Investigation of the geologic history of the northwestern Albuquerque basin began in the mid-1900s, but accelerated in the 1990s through today. Earliest investigations on the Santa Fe Group recognized three main stratigraphic units: the Upper buff, Middle red, and Lower gray members within the Santa Fe Formation (Bryan and McCann, 1937, 1938; Wright, 1946; Spiegel, 1961; Connell, 2008b). The lower gray was renamed as the Zia Formation (Galusha, 1966) and subdivided into three members (ascending order): Piedra Parada, Chamisa Mesa, and Cañada Pilares (Galusha, 1966; Gawne, 1981; Tedford, 1982; Tedford and Barghoorn, 1997). The stratigraphic nomenclature of Kelly (1977) proposed formalizing two members within the Santa Fe Formation: the Ceja member (formerly the Upper buff member) and the Zia member (downgrading the Zia Formation of Galusha, 1966, to member status). Black and Hiss (1974) made inferences regarding stratigraphy and structure from a deep oil well in the study area, the Shell Oil Co. Santa Fe Pacific No. 1 test well, including first documentation of the Ziana horst (which they referred to as the Ziana anticline).

Intensive geologic and geophysical investigations began during the early 1990s and continued through 2000-2010, contemporaneous with drilling of deep-water wells for the city of Rio Rancho and in western Albuquerque (Appendix 1; Allen et al., 1998; Connell et al., 1998). This round of geologic investigations included 1:24,000 geologic mapping (Cather et al., 1997; Connell, 1997; Koning et al., 1998; Koning and Personius, 2002; Personius, 2002; Personius et al., 2000; Thompson et al., 2009) that was synthesized and compiled at lower scales by Connell (2008a) and Williams and Cole (2007). Graduate student investigations of the sedimentology and petrography of the Santa Fe Group in the northwestern Albuquerque Basin include Lozinksy (1988, 1994), Gillentine (1994), Brandes (2002), and Smyth (2004). Interpretations of Santa Fe Group strata encountered in a deep oil well in the study area (the Tamara No. 1-Y well) are presented in Connell et al. (2001). Relatively up-to-date treatments of the lithostratigraphy of Santa Fe Group strata in the study area are given in Connell et al. (1999), Connell (2008b), and Connell et al. (2007). Thorough treatments of the geologic history of the Albuquerque basin, including age control, are provided in Connell (2004) and Connell et al. (2013). Geophysical interpretations of geologic structure include those containing seismic data (May and Russell, 1994, and Russell and Snelson, 1994), aeromagnetic data (Grauch, 1999; Grauch et al., 2001), and gravity data (Grauch et al., 1999). An essential publication of Albuquerque basin structure that integrates geophysical data and well interpretations is Grauch and Connell (2013). Mapping and paleoseismic data of Quaternary faults were compiled by Machette et al. (1998), and fault data from the Quaternary Faults and Folds database were used in our study (https://earthquakes.usgs.gov/hazards/qfaults). Studies of fault zone architecture in the Santa Fe Group in or near the study area include Minor and Hudson

(2006), Caine and Minor (2009), Rawling and Goodwin (2006), and Rawling et al. (2001). Recent geologic mapping efforts have focused in the Rio Puerco Valley and the nicely exposed badlands between Ceja del Rio Puerco and the Rio Puerco (Cikoski et al., 2012; Koning and Jochems, 2014; Koning and Rawling, 2017).

Detailed groundwater investigations in the northwestern Albuquerque basin generally began in conjunction with accelerated growth of Rio Rancho during the early 1990s. Most of these investigations involved evaluating newly drilled wells or planning new wells for the city (Appendix 1) or for northwestern Albuquerque (Allen et al., 1998; Connell et al., 1998). Comprehensive investigations of the hydrogeologic framework of the Albuquerque basin were initiated by Hawley and Haase (1992), Hawley et al. (1995), Hawley (1996), and Thorn et al. (1993). Groundwater temperature and hydrothermal studies were studied by Reiter (2001, 2003).

The U.S. Geological Survey conducted many noteworthy hydrogeologic studies in the Albuquerque basin during the 1990s and 2000s. These efforts included early groundwater flow modeling in the Albuquerque basin (Kernodle and Scott, 1986; Kernodle et al., 1987, 1995; and Kernodle, 1998). The U.S. Geological survey also spearheaded several geochemistry investigations: Sanford et al. (2004a, 2004b), Plummer et al. (2001, 2004a,b,c), Bexfield and Plummer (2003) and Bexfield et al. (1999). Plummer (2004a,b,c) used a variety of geochemical data to map out various groundwater hydrochemical zones for the upper 2,000 ft of the Santa Fe Group aquifer system (Fig. 11). Groundwater-level maps include those of Bexfield and Anderholm (2000, 2002), which indicated a curious north-south groundwater low (trough) feature west of the Rio Grande. These studies were used to make updated groundwater flow models relevant to our study area (McAda and Barroll, 2002; Bexfield et al., 2004) and assessment of groundwater resources (Bartolino and Cole, 2002). Minor and Hudson (2006) investigated how faults in the northwestern Albuquerque basin affect groundwater flow.

A consultant report by Glorieta Geoscience, Inc. (Riesterer et al., 2004) is particularly relevant to our study (Appendix 1). Riesterer et al. (2004) used available data from 35 production wells and piezometers to determine if there were geologic controls on well production and water quality. If so, these could be used to identify the most promising areas for future groundwater production. This effort involved making a structural contour map of the upper, middle, and lower subdivisions of the Santa Fe Group. Riesterer et al. (2004) concluded that the most important factors influencing well production were well depth and total length of screen, regardless of geologic unit or proximity to faults. Arsenic did not vary in a predictable manner, and water quality did not seem to decline with depth (up to 2,500 ft). Other

consultant reports from which we derived data for our study (such as pumping test and chemical data) are listed in Appendix 1.

Organization of Report

This open-file report is organized as follows. First, we provide the geologic setting of the study area, including the geologic structure and stratigraphy of the Santa Fe Group. Because it is used in many of the later analyses, how we constructed the potentiometric surface is discussed. We then treat the three main topics in our study: 1) 3D mapping of the Santa Fe Group aquifer (including mapping the tops of hydrostratigraphic units, the tops of the saturated parts of the hydrostratigraphic units, and associated isopach maps); 2) assessing permeability differences between and within HSUs; and 3) a preliminary treatment of spatial differences in total dissolved solids (TDS), which may be considered as an approximate groundwater quality proxy, as well as the spatial distribution of radiocarbon ages. For each of the three main topics, we include a methods and results section.

GEOLOGIC SETTING OF STUDY AREA

Geologic structure

The study encompasses much of the northwestern corner of the Albuquerque basin, one of the largest basins of the Rio Grande rift (Grauch and Connell, 2013). The Albuquerque basin can be subdivided into three sub-basins (listed from north to south): the Santo Domingo, Calabacillas, and Belen sub-basins (Fig. 3 reproduced from Grauch and Connell, 2013). The overall geometry of the Calabacillas sub-basin is asymmetric, deepening eastwards towards major west-down faults near the foot of the Sandia Mountains (Grauch and Connell, 2013). Two large-displacement, east-down, north-striking normal faults are present in the western part of the study area: the San Ysidro and Zia faults (Fig. 4). A graben lies between the Zia fault and the Ziana horst block (the horst is discussed below), merging to the south-southeast with the deeper portion of the Calabacillas sub-graben (Grauch and Connell, 2013). We informally refer to this graben as the “Montoyas graben” after the nearby geographic feature of Arroyo de Los Montoyas (Figs. 3-4). The graben is structurally deepest between the Zia fault and the west-down Doval fault.

An important structural feature in the northwest Albuquerque basin, found in the northeast part of the study area, is the south-plunging Ziana horst block, located east of the Montoyas graben (Figs. 3, 4). Note that this feature was previously referred to as an anticline (Black and Hiss, 1974) but detailed mapping indicates that the term "horst" is more appropriate in the southern part of the structure (Personius et al., 2000); we use "horst" in this report since it is clearly bounded on both sides by oppositely dipping faults, even though to the north the structure is folded into an anticline geometry (Koning and Personius, 2002; Riesterer et al., 2008, cross section B-B'). The Ziana horst is bounded on the west by the west- to southwest-down Coronado-Alameda fault, and on the east by a series of east-down, north-striking normal faults (listed from west to east): Arroyo Venada, Tamaya and San Felipe faults (Fig. 4). Southeast of the Ziana horst block, gravity data (Grauch and Connell, 2013) indicates a subdued structural high that extends southeastwards to the northern part of the Sandia Mountains. The Ziana horst and this southeast-trending structural high separate the Calabacillas sub-basin from the Santo Domingo sub-basin to the north and northeast (Fig. 3).

The manner in which layered rock is tilted (described by stratal strikes and dips) is critical for producing the 3D geologic model in this project and is obtained by inspection of previous geologic mapping (Fig. 4). Mapped strata dip 3-8° E on the footwall (west side) of the San Ysidro fault (Cather et al., 1997; Connell, 2008a). In the escarpment north of La Ceja, east of the Zia fault, strata have a strong southward component of dip (Koning et al., 1998; Koning and Personius, 2002; Connell, 2008a). Dips shallow (fan) up-section north of the La Ceja between the San Ysidro and Zia faults, from 5-7° S to 0-2° S between the Cerro Conejo Formation and the top of the Arroyo Ojito Formation (Koning et al., 1998). On the western flank of the Ziana horst, strata mostly strike north-northwest and dip 5-10° WSW. East of the Ziana horst, strata dip southerly and have NW, W, or SW strikes (Connell, 2008a). The complete structural picture of the study area is obtained by structural contouring of contacts using these attitudes and well picks, and will be discussed in the Results section of this report.

Santa Fe Group Lithostratigraphy and Hydrostratigraphic Units

Connell et al. (1999) synthesized investigations of the Santa Fe Group exposed north and west of Rio Rancho (Cather et al., 1997; Koning et al., 1998). Revisions of the Santa Fe Group nomenclature across the Albuquerque basin was published in Connell (2008a). A slightly different stratigraphy was proposed by Williams and Cole (2007). We follow the stratigraphic scheme of Connell (2008a) and summarize its

lithostratigraphic units below, in addition to discussing how hydrostratigraphic units relate to the lithostratigraphic units. Note that the terms “formation” and “members” relate strictly to lithostratigraphy, where rock units are recognized by physical attributes such as composition, texture, and color. A hydrostratigraphic unit, in contrast, is a zone (a layer in this study) in an aquifer that has unique physical properties pertaining to groundwater; these properties include permeability, porosity, yield, or hydraulic conductivity. The Santa Fe Group sequence hosting both these stratigraphic units is particularly well exposed north of La Ceja (Fig. 5) and west of Ceja del Rio Puerco. Figure 6 relates Santa Fe Group lithostratigraphic units with the hydrostratigraphic units devised in this study.

Zia hydrostratigraphic unit (Zia Formation, lower-middle Cerro Conejo Formation)

The lowest formation in the Santa Fe Group is a 300-3,000 ft (90-900 m) thick, sand-dominated succession called the Zia Formation (Fig. 6). We include all of the Zia Formation, plus the lower-middle Cerro Conejo Formation, with the Zia HSU (Fig. 6). The lowest unit of the Zia Formation, the Piedra Parada Member (Galusha, 1966), is primarily a medium- to coarse-grained, light-gray sandstone that is commonly cross-stratified (Fig. 7a); it ranges in thickness from 50-260 ft (15-80 m) near La Ceja to 1,280 ft (390 m) in the Santa Fe Pacific No. 1 well on the Ziana horst. The overlying Chamita Mesa Member (Galusha, 1966), 30-35 m thick west of the San Ysidro fault, is a light reddish brown to buff-colored, very fine- to medium-grained sandstone and silty sandstone (Fig. 7b) typified by medium to very thick, tabular beds that locally contain rhizoliths. West of Ceja del Puerco, the highest unit of the Zia Formation is the 30 m-thick Cañada Pilares Member (Gawne, 1981), which is characterized by reddish brown clay interfingering with very fine- to medium-grained sand tongues (Fig. 7b). These three members are interpreted to reflect a succession of the following paleo-environments: eolian + high-energy alluvial, distal piedmont slope, and playa + playa margins (Gawne, 1981; Tedford and Barghoorn, 1999; Koning and Jochems, 2014; Koning and Rawling, 2017). Available age control indicates a range of 22-16 Ma (Tedford and Barghoorn, 1999). The upper contact of the Zia Formation is a major unconformity or a compressed stratigraphic section west of the Zia fault, but is likely conformable on the southern hanging wall (east side) of the fault, particularly south of the latitude corresponding to the Ziana horst.

The lower–middle Cerro Conejo Formation is assigned to slightly reddish to orangish, tabular-bedded, mainly fine- to medium-grained sandstone and silty to muddy sandstone that locally make

prominent ledges (Fig. 7c), particularly near the La Ceja del Rio Puerco and north of Cerro Conejo (Fig. 4). The entire Cerro Conejo Formation is 1037 ft (316 m) thick north of La Ceja (where its type section is located; Connell et al., 1999) and 650-800 ft (200-250 m) thick west of Ceja del Rio Puerco (Koning and Jochems, 2014; Koning and Rawling, 2017). The formation likely thickens south and east of these exposures, respectively. In its type section, there is a cross-stratified, light-colored, fluvial sand unit 190-285 ft (58-87 m) above its base (unit 5 of Connell et al., 1999); this lower fluvial sand tongue is inferred to correlate to map unit Tcc3 of Koning and Jochems (2014), which is a 100-150 ft (30-45 m) thick interval of tabular-bedded to massive sand that contains an ash bed dated at 13.64 ± 0.09 Ma (Tedford and Barghoorn, 1999).

In well data, it is not possible to confidently pick the base of the Cerro Conejo Formation. However, the upper, sandy fluvial unit of the Cerro Conejo Formation can be differentiated in well data. Thus, the middle-lower Cerro Conejo Formation is lumped with the Zia Formation in our mapping of hydrostratigraphic units (HSU), but the upper Cerro Conejo Formation is assigned its own hydrostratigraphic unit (i.e., the Lower Rio Rancho HSU; Figs. 6, 7d).

Lower Rio Rancho hydrostratigraphic unit (upper Cerro Conejo Formation)

Of particular interest in our study is the upper Cerro Conejo Formation, corresponding to Unit 8 in the type section of Connell et al. (1999), which constitutes the Lower Rio Rancho HSU. The upper Cerro Conejo Formation is composed of cross-stratified to massive, fine- to coarse-grained sand with a notable paucity of mud beds (Fig. 7d). It extends across most of the study area but interfingers westward with a light red to light orange, thickly bedded, sandy piedmont facies called the Benavidez Member of the Cerro Conejo Formation (Fig. 8; Koning et al., 2021, note that future work by the lead author will likely assign the Benavidez Member to the Arroyo Ojito Formation); the inferred location of this interfingering boundary is close to the Zia fault, west of the well control in our study. The upper Cerro Conejo unit is nicely exposed along US 550, where it contains a white bed of 11.3 Ma Trapper Creek B tephra (Koning and Personius, 2002).

Middle Rio Rancho hydrostratigraphic unit (Navajo Draw and Loma Barbon Members of Arroyo Ojito Formation; Benavidez Member of Cerro Conejo Formation)

The Cerro Conejo Formation is gradationally overlain by gravel-bearing strata assigned to the Arroyo Ojito Formation (Figs. 6, 8, 9). With the exception of the Picuda Peak Member (Connell, 2008b), Arroyo Ojito strata are included in the Middle Rio Rancho HSU. The Arroyo Ojito Formation (>1,300 ft, >400 m thick) consists of sand, muddy sand, mudstone, and gravel beds that are mostly tabular-bedded, although coarse channel fills may be lenticular to broadly lenticular. Three lithostratigraphic units comprise the Middle Rio Rancho HSU (Fig. 8). To the west lies the Benavidez Member of the Cerro Conejo Formation (Koning et al., 2021), which generally lacks clay beds and mostly has a chert-dominated gravel fraction. The Benavidez Member represents deposition by high-energy, ephemeral streams and interfingers eastward with the Navajo Draw Member of the Arroyo Ojito Formation (Koning et al., 2021). The Navajo Draw exhibits a distinctive pale-yellow to pale-brown color (Figs. 9a-9b) and has a heterolithic gravel fraction dominated by volcanic rocks (to the north) and chert (to the south). This member represents deposition by a fluvial system (ephemeral or perhaps perennial) that drained the southeastern Colorado Plateau and the southeastern San Juan Basin (Connell et al., 1999); the yellow color of the sediment probably reflects erosion of Cretaceous strata in the structurally high area south of Cuba, southwest of the southern end of the Nacimiento Mountains. The Loma Barbon Member (Figs. 9c-9d) is reddish-yellow to strong brown and light-yellowish brown, and has a gravel assemblage dominated by granite, volcanic rocks, quartzite, and yellowish-brown or reddish-brown sandstones (Connell et al., 1999). Although the Loma Barbon Member interfingers westward with the upper Navajo Draw member, to the east it overlies the lower Navajo Draw Member. The Loma Barbon is interpreted to reflect deposition on a distal fan and adjoining basin floor by a paleo-Jemez River carrying detritus from an exhuming (eroding) Sierra Nacimiento (Connell et al., 1999); its red color may reflect erosion of former Triassic and Permian strata from the top of these mountains. Northeast of the study area, the Loma Barbon Member likely interfingers eastward with volcaniclastic strata shed from the Jemez Mountains (Cochiti Formation of Smith and Lavine, 1996). To the east of the study area, the Loma Barbon Member interfingers with ancestral Rio Grande fluvial strata (Connell et al., 1999). Arroyo Ojito strata tend to be slightly tilted and faulted and are relatively consolidated.

Upper Rio Rancho hydrostratigraphic unit (Ceja Formation)

The Upper Rio Rancho hydrostratigraphic unit comprises the relatively coarse-grained, Picuda Peak Member (Arroyo Ojito Formation) and the overlying Ceja Formation. The Picuda Peak Member is a pinkish gray to reddish, sandy gravel-gravelly sand unit conformably overlying the Loma Barbon Member

(Arroyo Ojito Formation) between the Zia fault and Ziana horst (Figs. 6, 8, 9e). Its gravel fraction is notably coarser than underlying Arroyo Ojito strata (table 2, Connell et al., 1999) and composed of red granite and Pedernal Chert, with lesser yellowish-brown sandstone, brownish-yellow chert, and quartzite (Connell et al., 1999; Koning and Personius, 2002). It is probably latest Miocene-early Pliocene, based on basalt clast $^{40}Ar/^{39}Ar$ ages of 6.5-8.3 Ma (Koning and Personius, 2002; table 2), which provide a maximum age of deposition for the unit. This coarse unit was called the Picuda Peak Member of the Arroyo Ojito Formation by Connell (2008b), but differentiating the top of this unit in well data proved very difficult. Thus, in our study the Picuda Peak unit is subsumed into the Upper Rio Rancho hydrostratigraphic unit.

The Plio-Pleistocene Ceja Formation includes three members that interfinger eastward with axial-fluvial facies of the ancestral Rio Grande. The axial-fluvial facies are included in the Sierra Ladrones Formation (Fig. 6). Near the Ceja del Rio Puerco, fine- to medium-grained, pink to light brown sand and minor clayey mudstone is assigned to the Atrisco Member. The Atrisco Member is overlain by grayish to tan, unconsolidated, gravelly sand and sandy gravel of the Rio Puerco Member (Fig. 6). The gravel of the Rio Puerco Member is composed of chert, 20-30% quartzite, and minor (<15% each) of intermediate-mafic volcanic clasts, sandstone clasts, and granite clasts. These two members are often recognizable in many wells found in the western study area but differentiation becomes more difficult to the east. Near the eastern study area boundary, reddish, relatively coarse sediment is assigned to the Santa Ana Mesa Member. The high proportion of arkosic sand in the Santa Ana Mesa Member and reddish color suggests it was deposited by the Rio Jemez in the late Pliocene to early Pleistocene. The Ceja Formation is ~300 ft (~100 m) thick.

POTENTIOMETRIC SURFACE

We constructed a potentiometric surface in order to map the top of saturated HSUs in our study and construct isopach maps of these saturated HSUs. Two terms related to groundwater levels, water table and potentiometric surface, warrant explanation. The **water table** is the elevation (or depth) of saturated sediment in relatively unconfined conditions. When penetrated by a well, the water level in the well would be approximately the same as the top of the saturated sediment. Under confined (artesian) conditions, however, the level of the water within the well casing could be notably higher than

the top-elevation of saturated sediment. The water level in a well that exists in either confined or unconfined conditions is called the **potentiometric surface**.

Previous mapping of the potentiometric surface was published by Kernodle (1998), reflecting groundwater conditions in the middle 1990s. We updated this map by compiling more recent groundwater levels (Table 1). Paucity of recent water-level data near the northern and western margins of the study area necessitated using older (1956-1984) water levels from stock wells. Water-level data for dates when a well seemed to be experiencing focused drawdown, presumably due to active pumping, were excluded. Depth to water measurements were converted to water-level elevations using a digital elevation model.

Contouring of the potentiometric surface was conducted using the following steps in ArcGIS's Spatial Analyst Tools. First, a natural neighbor surface interpolation was performed (Natural neighbor tool in Interpolation toolset) using the well data in Table 1 and spot elevations of the lower Rio Jemez and Rio Grande; for the latter, we assumed that groundwater depth is near-zero at these rivers. Second, the potentiometric surface was contoured (40 ft contour interval) using the Contour tool (Surface toolset), Third, the contours were edited according to topography and were extended manually in the northwestern part of the study area. These contours, water-level elevations in wells, and the elevations of the rivers were used as inputs for the ArcGIS tool called Topo to Raster. This tool was used to produce a xyz grid file of the potentiometric surface-elevation in the northwestern Albuquerque basin (127.4 m x 127.4 m grid size), which was smoothed utilizing the focal statistics tool (Neighborhood toolset in Spatial Analyst), where we used a 90degree wedge neighborhood setting with 3-cell search radius.

The Natural Neighbor interpolation is an Inverse Distance Weighted (IDW). In an IDW interpolation, measurements that are closest are given more influence on the predicted value than those farther away. Natural Neighbor interpolation differs slightly from IDW as it selects the input points that are closest to an interpolation point but then creates a convex hull around these points. The interpolation then weights their values by proportionate area. This method tends to create smoother, more realistic water tables that don't have dramatic cliffs or drop-offs, which rarely represent real-world water table geometry. This methodology also removes the need to specify parameters such as radius, the number of neighbors, or weights.

Maps of the depth to the potentiometric surface and potentiometric surface elevation are presented in Figures 10 and 11. Note that the input data for these maps were not as rigorously screened

as the U.S. Geological Survey's potentiometric maps produced for the neighboring city of Albuquerque (e.g., Galanter and Curry, 2019), as exemplified in our inclusion of water levels spanning decades of time. Therefore, this map should be considered as an "approximation" of the potentiometric surface, locally having up to 10-100 ft (3-30 m) of inferred vertical error, especially towards the northwest corner of the study area (i.e., where elevation-contour lines are dashed in Figure 11). The implications of the geometry of the potentiometric surface are discussed in the Results section below.

The potentiometric surface-elevation map can be used to infer groundwater flow paths, which flow perpendicular to the contour lines towards elevation lows (Fig. 11). The lowest elevations of the potentiometric surface lie in an elongated region between the western part of Paseo del Norte northward towards well RRU-19 near Southern Boulevard. This potentiometric surface nicely corresponds to the "groundwater trough" of Plummer et al. (2004a,c); explanations for its existence are evaluated in the Discussion section. The map geometry of the low is probably influenced, at least in part, by the pumping of wells NMU1, W-4, RRU-19, and RRU-6A, and its north-south elongation may be controlled by nearby, north-striking faults acting as groundwater barriers. Westwards across the Zia fault, for example, the potentiometric surface steps up ~40 ft (10-15 m). To the east of this low, potentiometric contours trend northeast; therefore, under the southeastern part of the study area groundwater likely flows to the northwest towards this potentiometric-surface low from the Rio Grande – consistent with a component of recharge from the Rio Grande. In the northern study area, the potentiometric surface slopes south-southwest from the Jemez River, but the lack of well control there makes the specific geometry of the surface there uncertain. The potentiometric surface forms a "mound" over the Ziana horst, suggestive of faults acting as barriers alongside the horst or fault-controlled, groundwater in-flow from the north between the unnamed, west-down fault near RRU-15 and the Arroyo Venada fault. Groundwater may possibly be upwelling near or north of RRU-23. There does not seem to be a strong slope in the potentiometric surface west of the Zia fault zone, and the exact configuration of the contours there is uncertain. We infer that groundwater contours there are likely orientated north-south due to possible barrier effects due to the San Ysidro and Sand Hill faults, but more data are needed to test that inference. Lastly, there appears to be a focused low in the potentiometric surface centered at RRU-9, which is likely due, in part, to pumping of that well (where water levels are demonstrated to be sensitive to pumping per consultant reports in App. 1) and relatively fine-grained, lower-permeability sediment there (discussed below).

3D-MAPPING OF HYDROSTRATIGRAPHIC UNITS WITHIN THE SANTA FE GROUP AQUIFER

Delineation of hydrostratigraphic units

In order to evaluate permeable trends and to identify possible "target aquifers," hydrostratigraphic units were formulated for the study area. Our initial scheme for delineation of hydrostratigraphic units (HSUs) was based on field observations conducted during extensive geologic mapping by the lead author (Koning et al., 1998; Koning and Personius, 2002; Koning and Jochems, 2014; Koning and Rawling, 2017). The first iteration envisaged the following grouping of lithostratigraphic units (listed in ascending stratigraphic order): Zia Formation; lower-middle Cerro Conejo Formation; upper, sandy Cerro Conejo Formation; lower, sandier Arroyo Ojito Formation, lower-middle, mud-rich Arroyo Ojito Formation; upper, coarser Arroyo Ojito Formation; and Ceja Formation.

To successfully create the 3D, subsurface geologic model, these hypothesized, initial HSUs needed to be recognized in well data and correlated between wells. For this purpose, we used the set of wells listed in Table 2, most of which had high-quality wireline data and archived cuttings (Appendix 2). Kingdom software was heavily employed in this initial evaluation of HSUs. This powerful software, developed for the oil industry, facilitates subsurface correlation of strata and vertical trends in porosity and clay content. Digital files of wireline (down-hole geophysical) data were used to make picks based largely on proportion of clay, which imparts a strong influence on permeability and also is measured in many wireline methods. Most wireline data were in hard copy format only, so time and effort had to be spent on translating these to a digital format. Lithologic textures and compositions in a well, based solely on cuttings data, were assigned numeric codes and used in the Kingdom analyses. Cuttings description data was obtained from consultant reports (Appendix 1) except for several wells whose cuttings were archived in the NM Bureau of Geology Cuttings Library, which the lead author described in detail (Appendix 3). Useful wireline curves proved to be resistivity and gamma-ray, density-porosity, and neutron-porosity (Fig. 12). Comparison of gamma-ray curves (particularly spectral gamma-ray curves) with cuttings suggested that the proportion of granite vs. non-granite cuttings seemed to have little influence on the gamma-ray curves; rather, the gamma-ray signal mostly reflected the amount of clay in the sediment. Using Kingdom software, Vshale ratios (i.e., the proportion of clay vs. total sediment) were also used to pick and correlate potential HSUs. Vshale ratios were calculated by comparing the magnitude of the gamma ray signal in inferred clay-dominated intervals vs. the magnitude of the gamma signal for relatively clay-free sand formations (note that depth intervals of sand vs. clay were inferred using cuttings and resistivity + neutron curves; Appendix 4). Using Kingdom software, one can plot the

various datasets for each well (i.e., various wireline curves plotted as a function of depth, cuttings lithology as a function of depth) and then compare wells side by side along chosen cross section lines (Fig. 12). One can then determine if certain subsurface intervals can be correlated between wells and that no drastic thickness changes occurred between wells that could not be accounted for by mapped faults. Sometimes changing picks in wells resulted in successful correlation of a given stratigraphic interval. The final lithologic picks (listed as ft-elevations) of units that could be correlated in the subsurface are presented in Table 2.

About a dozen Kingdom cross sections were made that allowed determination of which subsurface units could be correlated in subsurface. Since these units had different geophysical properties related primarily to the proportion of clay, and since clay directly impacts the degree of permeability, we considered these correlative units as potential hydrostratigraphic units; whether these HSUs indeed had unique permeability properties was later tested by compilation of hydraulic conductivities derived from pumping test data. The final hydrostratigraphic units are as follows (listed in descending stratigraphic order, and with lithostratigraphic counterparts listed in parentheses): **Upper Rio Rancho HSU** (Ceja Formation, Picuda Peak Member of Arroyo Ojito Formation); **Middle Rio Rancho HSU** (Navajo Draw and Arroyo Ojito Members of Arroyo Ojito Formation; Benavidez Member of Cerro Conejo and Arroyo Ojito Formations; **Lower Rio Rancho HSU** (upper, sand-dominated Cerro Conejo Formation and Benavidez Member); and the **Zia HSU** (lower-middle Cerro Conejo Formation containing notable muddy beds, and the entire underlying Zia Formation). Note that the lower-middle Zia Formation, corresponding to the sand-dominated Piedra Parada Member, seems to extend across the northern study area (based on its identification in the Santa Fe Pacific 1, Santa Fe Pacific 3, and Tamara wells), and could be a potential fifth HSU. We lumped this sandy, lowermost Santa Fe Group unit within the Zia HSU because of its great depth and general lack of penetration by existing water wells. The initially hypothesized lower Arroyo Ojito Formation HSU and lower-middle, muddier Arroyo Ojito HSU could not be successfully correlated across the study area and thus were subsumed into the Middle Rio Rancho HSU (Figs. 6, 8). In most areas, the Arroyo Ojito Formation coarsened upward, but the lower boundary of this coarsening is too diffuse to correlate between wells.

Subsurface Mapping Methods

Mapping HSU tops (includes both saturated and unsaturated zones)

The final geologic model consists of a set of raster surfaces, each of which corresponds to the top of one of the four HSUs (Plates 1-4; Appendix 5). These raster surfaces were made using an ArcGIS tool called Topo-to-Raster, whose inputs were elevations of the HSU tops in the 30 studied wells and structural contours. The well picks were already determined using the previous analyses involving Kingdom lithologic picks and inter-well correlations. Below, we summarize how the structural contours were constructed for the tops of the Zia, Lower, and Middle Rio Rancho HSUs. More detail about the ArcGIS component of the methodology is given in Appendix 6.

Except for the Upper Rio Rancho HSU, the lithostratigraphic-top equivalent of a given HSU was identified in outcrops north of La Ceja. The top contact of the Upper Rio Rancho HSU corresponds to surface topography and thus did not need to be identified in outcrop. These lithostratigraphic tops (*per HSU unit*) were: top of the Loma Barbon Member or, if absent, Navajo Draw Member of the Arroyo Ojito Formation (Middle Rio Rancho HSU), top of the Cerro Conejo Formation (Lower Rio Rancho HSU), and the top of the ledge-forming, reddish, middle part of Cerro Conejo Formation (Zia HSU). The last contact had to be drawn in using aerial imagery, but the other contacts were already mapped (Cather et al., 1997; Koning et al., 1998; Koning and Personius, 2002).

Using data from these earlier maps, compiled in Connell (2008a), structural contours were drawn southwards from the La Ceja outcrops and eastward from Ceja del Puerco outcrops. Attitudes from geologic maps, lithologic picks in wells (Table 2) and locations of major faults were essential for drawing structural contours away from outcrops. Major faults, defined as those with vertical offsets of more than about 300 ft (100 m), were explicitly modeled by drawing structural contours of their associated fault planes, beginning with their mapped ground trace and extending down-dip according to dip values shown on the geologic map of Connell (2008a). Where no dip data existed, we assumed a dip value consistent with those measured on nearby faults. Faults that were incorporated into the 3D hydrogeologic map include: San Ysidro fault, Zia fault, Doval fault, Coronado-Alameda fault, an unnamed, east-down fault between the Doval and Coronado-Alameda fault, Arroyo Venada fault (new name), Tamaya fault, and the Santa Ana section of the San Felipe fault. Vertical displacements for a given fault, used to offset the HSU structural contours, were determined by apparent offsets of strata in the Kingdom software cross sections as well as vertical displacements calculated from offset contacts on the geologic map of Connell (2008a).

Rasters were generated separately for the tops of the Middle Rio Rancho HSU, Lower Rio Rancho HSU, and the Zia HSU. These tops incorporated both the unsaturated and saturated parts of a given HSU

559 and are found in the feature dataset called “HydroStratUnits_tops” (Appendices 5, 6). For the tops of
560 the Middle and Lower Rio Rancho HSUs, as well as the Zia HSU, “relative accuracy” polygons were drawn
561 in areas that we judged contained poor well control (contained in the AccuracyPolygons feature dataset
562 in the geodatabase of Appendix 5). For all three HSUs, low-accuracy polygons are present on the
563 hanging wall (east side) of the Tamaya fault. For the Lower Rio Rancho HSU and Zia HSU, a low-accuracy
564 polygon extends across most of the southern one-fifth of the study area. Caution should be used when
565 making interpretations of the data in these areas as the uncertainty in the results is higher there.

566 **Mapping saturated-HSU tops**

567 Mapping the top of the saturated portions of a given HSU is more involved than mapping the entire
568 HSU. Two zones within an aquifer need to be considered: 1) the zone where the HSU is completely
569 saturated (extending from the top to lower contact of the HSU), and 2) the partially saturated zone,
570 which in the study area is locally found on the western and northern periphery of the completely
571 saturated zone of an HSU. In the partially saturated zone, the elevation of the potentiometric surface
572 lies below the top of the hydrostratigraphic unit.

573 Working from the Zia HSU upwards to the Upper Rio Rancho HSU, we first define the saturated
574 extent of a given HSU. Then, within that saturated extent, we combine two rasters to obtain the top of
575 the saturated zone: (1) a raster showing the HSU top where it is fully saturated (corresponding to the
576 HSU top in the previous section), and (2) a raster containing the elevation of the water table where the
577 HSU is partially saturated. See Appendix 6 for the ArcGIS details related to this procedure.

578 **Creating Isopach maps**

579 An isopach map shows the thicknesses of a given map unit by means of color-shading and/or
580 contour lines. Two types of isopach maps were created, the details of which are given in Appendix 6. The
581 first incorporates the entire thickness of an HSU, containing both saturated and unsaturated strata. It is
582 created by subtracting a raster containing the elevations of the base of an HSU from a raster containing
583 the elevations of the top of an HSU. The second isopach map only calculates the thickness of the
584 saturated intervals of an HSU. In the associated raster calculations, one subtracts the saturated base of
585 an HSU (corresponding to the saturated top of the underlying HSU) from the saturated top of the HSU.
586 These surfaces are the same as the rasters used to map the saturated tops of HSUs (a discussed in the
587 previous section).

588

Results

Extent and geometry of HSUs

Sixteen plates in this OFR illustrate the geometry and elevations of the bounding surfaces of the mapped hydrostratigraphic units, in addition to illustrating their thickness variations. Plates 1-8 pertain to the entire hydrostratigraphic unit, including both its saturated and unsaturated portions. Plates 9-16 only depict the bounding surfaces and thicknesses of the saturated zone of the hydrostratigraphic units. Plate 17 illustrates which HSUs are present at the potentiometric surface. The ArcGIS map package containing the HSU rasters and other features depicted in the plates (like structural contours) is provided in Appendix 5. Figures 13-14 show the elevation-contoured upper surfaces of the Middle and Lower Rio Rancho HSUs, and Figures 15-17 depict the elevation-contoured tops of the saturated zone contained within the Upper, Middle, and Lower Rio Rancho HSUs, respectively. Figures 18-19 are isopach maps of the saturated Upper and Middle Rio Rancho HSUs, respectively.

We synthesize these data regarding the subsurface geometry of the hydrostratigraphic units using a three-dimensional block diagram (Fig. 20). The southern and eastern faces of this diagram correspond to the cross-section lines shown in Fig. 4 (blue lines labeled A-A' and B-B'). Figure 21 provides a 3D depiction of the HSU surfaces. Both these illustrations (Figs. 20 and 21) illustrate thickness variations between the HSUs (for example, the Lower Rio Rancho HSU is notably thinner than the Middle Rio Rancho HSU), how they are offset by faults, and the Ziana horst block.

Hydrogeologic implications

Here we discuss important hydrogeologic features in the study area, starting in the northwest of the study area and moving counter-clockwise.

Western faults

The San Ysidro and Zia faults play major roles in the hydrogeology on the west side of the study area. About 100-1,000 feet (30-300 m) of east-down, vertical displacement of HSU surfaces occur across these two structures. The top of the Lower Rio Rancho HSU (corresponding to the base of the Middle Rio Rancho) is commonly offset more than the top of the Upper Rio Rancho HSU. (Figs. 13-14). The saturated Middle Rio Rancho aquifer is generally only present on the east side of the San Ysidro fault and thickens notably east of the Zia fault, where it is ~3000 ft (~900 m) thick south of Southern Boulevard (Fig. 19).

Montoyas graben

Between the Zia fault and the Ziana horst is a structurally depressed area, referred to as the Montoyas graben (after the nearby Arroyo de los Montoyas), bisected by the west-down Doval fault (Figs. 16, 17, 19). East of the Doval fault, map data (Connell, 2008a) indicate NNW strikes and WSW dips, so the eastern part of the graben is modeled as a ~3°, WSW-dipping homocline. A ~100 to few hundred feet (30 to ~100 m) of west-down offset is inferred to occur along the Doval fault, so the deepest part of the Calabacillas graben is modeled as a narrow (~2 mi, 3 km wide) arm bracketed between the Doval and Zia faults (Figs. 14, 17). It is in this arm that the saturated Middle Rio Rancho HSU is estimated to be 2,000 ft (600 m) thick (Fig. 19).

The Montoyas graben merges with the Calabacillas sub-basin close to the south end of the Doval fault, near the western end of Paseo del Norte (Figs. 14, 17). South of Southern Boulevard, the saturated Upper Rio Rancho HSU is preserved, increasing southward in thickness to roughly 500-600 ft (150-180 m) thick on the hanging wall (east side side) of an unnamed fault paralleling ~~Uni~~verse Boulevard (Fig. 18). This fault is inferred largely from an aeromagnetic lineament (Connell, 2008b) and the top-of-bedrock surface in Grauch and Connell (2013). The amount of throw across this fault is uncertain, so there is considerable uncertainty in how much the saturated Upper Rio Rancho HSU thickens across it. The underlying saturated Middle Rio Rancho HSU is estimated to be roughly 3,000–4,000 ft (900–1,200 m) thick in the area east of this unnamed fault, but that thickness is poorly constrained. Note that the sandy Lower Rio Rancho HSU may not extend as far south as this area, in the sense of being unique compared to the Zia HSU in texture and permeability, (Fig. 17; Plates 3, 6), based on the apparent absence of this HSU in the Black Ranch Test Well (Table 2; BR on Figures 14-19).

Southeast corner of the study area

Data from abundant wells indicate relatively steep southward dips of the Upper / Middle Rio Rancho HSU contact near the eastern end of ~~Sou~~thern and Northern Boulevards. The related structure was called the Loma Colorado Transition Zone in Hawley and Whitworth (1996). This structure defines the southern end of the Ziana horst (see below) and results in the Middle Rio Rancho HSU being thicker to the south (Fig. 19).

Based on this structure and the top-of-bedrock surface of Grauch and Connell (2013), we infer that the Santa Fe Group aquifer is thickest in the southeast corner of the study area, in the vicinity of the intersection of Coors Boulevard and Paseo del Norte (Figs. 18-19). Here, the saturated-Upper Rio Rancho

HSU is 1,500-1,800 ft (450-550 m) thick, and the underlying saturated Middle Rio Rancho HSU is inferred to be greater than 4,000 ft (>1200 m) thick. The saturated Upper Rio Rancho HSU decreases in thickness to the north, between the unnamed fault near Universe Boulevard and the Coronado-Alameda fault, pinching out northwards about midway between Southern and Northern Boulevards along the aforementioned Loma Colorado Transition Zone (Fig. 18). The Zia HSU is also probably thick in the southeast corner (Plate 8), but as noted earlier we are not certain whether the sandy Lower Rio Rancho HSU extends further south than Southern Boulevard as a distinguishable unit from the Zia HSU (Fig. 17; Plate 3). Except for the Lower Rio Rancho HSU, the thickest saturated-HSUs, and correspondingly the highest aquifer transmissivities, are interpreted in the southeast corner of the study area.

Coronado-Alameda fault

The fault that bounds the western and southwestern side of the Ziana horst is inferred to be a continuation of the Coronado-Alameda fault (Connell, 2008a). That such a SW-down normal fault is present is well-supported by our lithologic picks and inter-well correlations in the area west of NM-528 (northern Coors Boulevard) and north of Southern Boulevard. Based on these correlations, we interpret that several hundred feet of southwest-down vertical displacement on the Coronado-Alameda fault, increasing to the southeast. The saturated Upper Rio Rancho HSU is interpreted to increase in thickness by 400 to 800 ft (120-250 m) across this structure (from NE to SW), and thus the fault should be considered as an important hydrogeologic feature that forms the northeastern side of relatively thick, saturated Upper Rio Rancho HSU (Fig. 18).

Ziana horst

The Ziana horst (referred to as the Ziana anticline in Black and Hiss, 1974), extends southeasterly across the east-central part of the study area (Fig. 4, 13-21). It is bounded mainly by the aforementioned, WSW-down Coronado-Alameda fault and a series of east-down faults that include the Arroyo Venada, Tamaya, and San Felipe faults. To the north of Rio Rancho, the Coronado-Alameda fault appears to die out northwards, and the western margin of the Ziana horst is mainly a WSW-dipping homocline merging westward with the eastern Montoyas graben. Many internal, relatively small-displacement faults are present within the delineated horst block, which form a particularly complex network near Rio Rancho High School, between the eastern ends of Northern and Southern Boulevards (Fig. 4). In order to reconcile geometries during the structural contouring of HSU tops, we reinterpreted the mapping of the two innermost faults of the Ziana horst (cf. Personius et al., 2000; Connell, 2008a).

The western of the two faults (unnamed) continues northward from previously mapped faults near RRU-22 and RRU-10; our contouring effort east of RRU-16P necessitated this fault being west-down there, and it is connected to previously mapped west-down faults near RRU-15 and SFP-1 (Fig. 2; Figs. 13-19). The eastern of the two inner faults is a large east-down fault immediately west of RRU-18 (Fig. 4), which we call the Arroyo Venada fault (new name), the majority of which was mapped earlier by Personius et al. (2000). An ash located at the bottom of the RRU-18 well (2,070-2,080 ft depth) chemically correlates with an 11.3 Ma Trapper Creek B Ash (Appendix 7). This ash is more or less at the same stratigraphic level as the 11.19±0.10 Ma Trapper Creek ash seen in outcrop along Highway 550 (sample MRGB-19BN of Koning and Personius, 2002), and together these ashes provide a stratigraphic datum for mapping the top of the Lower Rio Rancho HSU across this fault. Our structural contouring of this datum indicates several hundred feet of east-down vertical displacement on the Arroyo Venada fault, which must have occurred after emplacement of the 11.2-11.3 Ma Trapper Creek ashes.

On the Ziana horst, the tops of the hydrostratigraphic units strike east-northeast and dip south-southeast (e.g., Fig. 14). Furthermore, the Upper and Middle Rio Rancho HSUs pinch out to the north-northwest on this horst (Plates 5-8). This results in a north-northwest pinch out of the saturated parts of these particular HSUs (Figs. 15–16, 18-199). The saturated Upper Rio Rancho HSU is generally restricted to the southeast of NM 528 (Fig. 19). The saturated Middle Rio Rancho HSU extends only about 3 miles (5 km) north of the RRU-10 and RRU-10A wells on the footwall (west side) of the Arroyo Venada fault. However, it continues several kilometers northward on the west side of the unnamed fault extending from RRU-10 to RRU-15, where it is 600-1000 ft (180-300 m) thick and thickens to 800-1,500 ft (250-450 m) west of the Coronado-Alameda fault (Fig. 19). Between the Arroyo Venada and Tamaya faults, the saturated Middle Rio Rancho HSU is only a few hundred feet (~100 m) near US 550, but increases in thickness southwards to be >1000 ft (>300 m) thick near NM 528 (Fig. 19).

Bernalillo area, east of the Tamaya fault

Because of their long lengths, we assume several hundred feet of vertical offset for each of the Tamaya and San Felipe faults (Santa Ana section). This is consistent with the interpretation that none of the studied wells east of the San Felipe fault fully penetrate the Upper Rio Rancho HSU (Table 2; Appendix 2). Due to this lack of penetration, HSU tops and saturated thicknesses for the Middle Rio Rancho HSU and lower units are uncertain.

ASSESSING PERMEABILITY DIFFERENCES BETWEEN AND WITHIN HSUs

We used two approaches to assess permeability differences between HSUs. The first entailed detailed mapping of selected vertical outcrop faces associated with a given HSU, and the second involved compilation of pumping test data reflective of permeability, namely hydraulic conductivities and specific capacities.

Outcrop mapping

Strata comprising the four HSUs are visible at the surface ~13 ~~miles~~ (20 km) to the northwest of the city, allowing direct study of the lithologic character of these HSUs in the badlands of the Zia Pueblo south of Highway 550 (Fig. 5). Direct study of the outcrops in this area allows for a comparative, local assessment of the lithologic differences between various stratigraphic intervals of the Santa Fe Group aquifer (i.e., between HSUs), and presumably these differences would also exist to the southeast in the subsurface. Collectively, these data can be used assess which HSUs may provide more favorable groundwater yields or hydraulic conductivities. Comparable outcrop analog studies for assessing aquifer permeability properties include those of Aigner et al. (1996); Al-Ajmi et al. (2011), Becker et al. (2019); Biteman et al. (2004); Busch et al. (2022); Davis et al. (1993); Gaud et al. (2004); Hornung and Aigner (2006); Howell et al. (2014); Keller et al. (2019); Klingbeil et al. (1999).

Only outcrops correlative to the upper Zia HSU and the Middle Rio Rancho HSU provided adequate vertical faces extensive enough for outcrop mapping, so we restricted our mapping to these two units. The studied upper Zia HSU corresponds to the middle Cerro Conejo Formation and the studied Middle Rio Rancho HSU includes outcrop faces of the Loma Barbon and Navajo Draw members of the lower-middle Arroyo Ojito Formation. Various data relating to this effort, including lithologic-texture maps of outcrop faces, are contained in Appendix 8.

Methods

At six sites (ZP-1 through ZP-6), depicted in Figure 2, we used an unmanned aerial vehicle (UAV) to photograph illustrative outcrops for both the middle-Cerro Conejo and lower-middle Arroyo Ojito Formations. Highly overlapping photographs with GPS coordinates taken from the UAV were stitched together using structure-from-motion software (Drone2Map) to produce 3D point clouds of the near vertical cliff faces that expose the units of interest. The 3D outcrops were mapped using ArcGIS software

to calculate relative proportions of sand vs. clayey sediment as well as sand amalgamation ratios (length of sand-against-sand contacts vs total contact length). The 3D models (Appendix 8) were used to measure lengths and thicknesses of sand bodies.

Results

Appendix 8 contains data related to the outcrop mapping effort. A text file (Appendix 08_TextFile) reviews the purpose of the study, procedures and results of the study. Tables A8-1 through A8-4 tabulate the measurement data from the annotated outcrops of the 2-D exposures. The annotated versions of the high-resolution, stitched images of the outcrop mapping are in a folder called called AnnotatedOutcropPhotos. The Appendix 8 folder called GeodatabasesForOutcropImages have geodatabases for each of the studied outcrops; these geodatabases contain spatial information (including metadata) of the flight lines and flight area and details regarding imaging processing. In these data, the upper Zia Formation HSU corresponds to the middle Cerro Conejo lithologic unit. The Stratigraphic lithologic intervals of the Middle Rio Rancho HSU include the Navajo Draw and Loma Barbon Members of the Arroyo Ojito Formation. Note that the two outcrop faces we studied in the Loma Barbon Member are from the lower part of this lithostratigraphic unit.

Compared to the analyzed Middle Rio Rancho HSU, the upper Zia HSU has higher proportions of sand (93-100% vs. 76-91% in the Middle Rio Rancho HSU), and lower proportion of clayey beds (<10% vs. 9-24% in the Middle Rio Rancho HSU) (Table 3). Sand amalgamation ratios are also notably higher for the upper Zia HSU (0.7-1.0) compared to the Middle Rio Rancho HSU (0.2-0.7), implying more connectivity of sandstones that would facilitate groundwater flow. Data from three sites suggest that the Loma Barbon Member has shorter clay body and sand body lengths compared to the Navajo Draw Member. Although the lower part of the exposed Loma Barbon Member (analyzed by this method) has ~10 percent clays, qualitative observation of outcrops and wells indicates that the Loma Barbon Member generally coarsens up-section so the clay percentage likely decreases up-section. Length measurements for sands are of limited practical value (for comparing the upper Zia HSU vs. the Middle Rio Rancho HSU) because they generally correspond to outcrop length. Clay lengths in the upper Zia HSU are longer than those in the Middle Rio Rancho HSU, by a factor of 3-4, based on four data points (sites). That would suggest higher connectivity between sand intervals in the Middle Rio Rancho HSU than implied by the sand amalgamation ratio (Table 3). Average sand body thicknesses are ~16 ft (5 m) in both the upper Zia HSU and the Middle Rio Rancho HSU, although locally in the upper Zia HSU they are as much as 55 ft (17 m). Collectively, these outcrop data suggest that the upper Zia Fm has lithologic

768 characteristics conducive to slightly higher permeability and groundwater yields. However, because the
769 Zia HSU was buried to a greater extent than the Middle Rio Rancho HSU in the Rio Rancho area, it is
770 expected to be more highly compacted and perhaps more cemented, and this will adversely affect its
771 permeability. Overestimation of actual permeability in subsurface strata has been documented in
772 previous outcrop analogue studies due to lower degrees of cementation and compaction in outcrops
773 compared to subsurface (well samples) (Busch et al., 2021). Furthermore, we only studied outcrop faces
774 representing limited stratigraphic intervals of either the upper Zia HSU and the Middle Rio Rancho HSU,
775 so extrapolating results to the entire hydrostratigraphic ~~unit~~ could very well be misleading.

776

777 **Determining sand vs. clayey sediment for HSUs using well data**

778 **Methods**

779 ***Well wireline analyses***

780 Rio Rancho has the fortune of having at least 38 wells with detailed well records (Appendix 2), 30 of
781 which were used for the structural contouring effort described earlier (Table 2). These well records
782 include archived cuttings and wireline geophysical logs. The wireline logs commonly containinduction
783 (or electric resistivity), spontaneous potential (SP), gamma ray, neutron porosity, and density porosity
784 data. Some wells have formation-analysis logs, the latter using the previously listed wireline data to
785 calculate sand vs shale vs calcium carbonate content as well as effective porosity as a function of depth.

786 Using these wireline data combined with available cuttings data, we delineated sand, clay, and
787 clayey sand intervals for 22 of these wells (Appendix 4). In terms of procedure, various well logs were
788 placed on a large Adobe Illustrator gridded canvas and adjusted so that they lined up side-by-side in
789 terms of depths. The utilized well logs included induction (or electric resistivity)+SP, gamma
790 ray+neutron-porosity, caliper+density-porosity, and formation-analysis (the latter only available for
791 wells RRU-10, RRU-6A, RRU-9, and RRU-14 through RRU-20). Curves of gamma-ray and conductivity,
792 digitized as part of the Riesterer et al. (2004) effort, were also placed on the canvas. Using standard
793 wireline interpretation methods to recognize subsurface lithologies, uniquely colored rectangles were
794 drawn in Adobe Illustrator that corresponded to sand vs clay intervals. “Muddy sand” was assigned to
795 depths not designated as sand or clay. The stack of colored rectangles allow for rapid visual assessment
796 of vertical changes in lithology in a given well. Depth ranges of each colored rectangle were tabulated

into an EXCEL spreadsheet. The proportions of clay, muddy sand, and sand were then calculated and compiled for each hydrostratigraphic unit (Table 4; Appendix 4).

Note that this lithologic break-out was conducted from the water table to the bottom of the well. Thus, the lithologic summaries only pertain to the saturated zones of a HSU; in the case of the Middle Rio Rancho HSU, which coarsens upwards, this will result in an underestimation of the sand content over the entire HSU (including the saturated and unsaturated zones). Also, for deep exploratory wells we only delineated lithologies to the bottom of the Cerro Conejo Formation in the case of deep oil exploratory wells.

Vshale analyses

Assuming higher percentages of sand correlates with higher permeability (Fetter, 2018; Gaud et al., 2004, fig. 3), an indirect method of assessing permeability changes is noting vertical or horizontal changes in the percentage of sand bodies in a hydrostratigraphic unit. As an ancillary to the aforementioned sand percentage dataset determined by detailed investigation and analysis of several wireline logs (Table 4, Appendix 4), we use solely gamma-ray data to calculate net-to-gross ratios of sand bodies relative to the saturated HSU thickness in a given well. This ratio can be viewed as a sand-body percentage, and is calculated using Kingdom software from down-hole gamma-ray logs. From the gamma-ray log, a Vshale curve is calculated using the end-members of pure-sand (approximate minimum of gamma-ray values) and pure-clay (approximate maximum of gamma ray values). The corresponding equation (Tearpock and Bischke, 2002) is:

Vshale = (GR-GRCLN)/(GRSHL-GRCLN)

where:

GR is gamma-ray log value at a measured depth

GRCLN is minimum gamma ray value (clean sand) along the studied depth of the well

GRSHL is maximum gamma ray value (clay or shale) along the studied depth of the well

For this study, sand bodies were recognized as such where the Kingdom Vshale value was 0.25 or less.

Results

Well wireline analyses

We used all available downhole wireline logs coupled with study of archived cuttings to manually delineate sand, clay, and clayey sand intervals for 22 wells in the study area. The proportions of sand vs. clayey sand vs. clay are tabulated in Table 4. Figure 22 summarizes the results of these analyses.

These data show that the Lower Rio Rancho HSU has the most favorable lithologic permeability proxies, followed by the Upper Rio Rancho HSU. The sand vs. clay ratio in the Lower Rio Rancho HSU is 17.1, that of the Upper Rio Rancho HSU is 4.4, whereas the Middle Rio Rancho and upper Zia HSUs are close to 3 and 2, respectively (Fig. 22). The proportion of clay and clayey sand in the Lower Rio Rancho HSU is at least half of that in the other three HSUs. The proportion of clay and sand (relative to total) in the Upper Rio Rancho HSU is 0.11 and 0.51, respectively, while that of the Middle Rio Rancho HSU is 0.16 and 0.47, consistent with possibly higher permeabilities for the Upper Rio Rancho HSU based on these lithologic proxies.

Going into this project, we had hypothesized that sand would increase and clay decrease to the northwest, parallel to paleo-streamflow (paleoflow data from Connell, 2008a, 2008b; Koning et al., 1998; Cather et al., 1997; Koning and Jochems, 2014; Koning and Rawling, 2017). However, such a trend is not obvious in most of the lithologic-texture data, at least not in the saturated zones of the Upper Rio Rancho and Middle Rio Rancho HSUs (Figures 23, 24).For the saturated part of the Upper and Middle Rio Rancho HSUs, the proportion of clay, muddy sand, and sand obtained from these analyses are plotted as pie charts on a map of the central study area (Figure 23). For a given well, the proportion of sand vs. clay in the Upper Rio Rancho HSU is consistently much more than that in the Middle Rio Rancho HSU, indicating a vertical trend in the data. To test our hypothesis regarding an upstream-orientated lateral trend, we orthogonally projected the sand and clay percent data of a well (shown in Figure 23) to a line trending 315° (upstream). The wells are divided into three sets according to what major structural zone they lie in: west of the Zia fault, within the Montoyas graben, and on the Ziana horst. The strongest lateral trend showing coarsening along a 315° trend corresponds to wells on the Ziana horst. A weaker trend is seen west of the Zia fault, where sand increases along a 315° direction but clay percentage is steady. Note that the rightward increasing separation (vertically) of the trend lines in both of these datasets corresponds to slightly higher sand vs clay ratios in an upstream direction. There is not notable trend in the Montoya graben. The fining that one observes in well data from east to west across the Zia

fault (from the Montoyas graben well set to the well set west of the Zia fault) may be due to the combination of a westward-decreasing groundwater table and down-dropping, on the east side of the fault, of coarser-grained strata in the upper part of the coarsening-upward Arroyo Ojito Formation. The lack of a clear lateral trend may perhaps be attributed to the extent of the study area being relatively minor compared to the entire length of the paleostream drainages (paleodrainage extent is not constrained to the northwest).

Storage zone thickness equates to sand body thickness and is shown via a box-and-whisker plot at the top of Figure 25. The Lower Rio Rancho HSU has the highest storage zone thicknesses (10 ft median vs. 6 ft median in the Upper Rio Rancho HSU). The median value of storage zone thickness is higher in the Upper Rio Rancho HSU than the Middle Rio Rancho HSU (6 vs. 4 ft), and ~50% of the data in the Upper Rio Rancho HSU have higher thickness values than ~75% of the data in the Middle Rio Rancho HSU. (i.e., the "boxes" in the plots). One can also consider the storage zone thickness as consisting of sand and muddy sand lying in-between clay beds (bottom of Fig. 25). Using this definition, the Lower Rio Rancho HSU has similar storage zone values than the Upper Rio Rancho HSU (e.g., 24 median vs.22 median), and the Upper Rio Rancho HSU has somewhat higher values and ranges than the Middle Rio Rancho HSU (e.g., 22 median vs. 8 median). The Middle Rio Rancho and upper Zia hydrostratigraphic units have comparable storage zone thicknesses using either definition, which contrasts with the outcrop-mapping results (upper right of Fig. 25). Because of the larger sampled stratigraphic intervals associated with the well ~~data~~ compared to the outcrop faces , we prefer the interpretation that permeability-related proxies are similar between the upper Zia and Middle Rio Rancho hydrostratigraphic units (e.g., compare the two units in Figs. 23 and 25).

Determining sand vs. clayey sediment for HSUs using Vshale analyses and density-porosity analyses

Where adequate gamma ray curves were available, net to gross sand body ratios were calculated for each saturated HSU, where sand bodies were delineated using a Vshale ratio of ≤ 0.25. These ratios equate to the proportion of sand bodies (relative to the total sediment) for a HSU in a well. On these same sand bodies in a given well (where Vshale ≤ 0.25), we also did a calculation of porosity using density-porosity wireline data.

Results of the Vshale and density-porosity analyses for the saturated zones of the HSUs are tabulated in Table 5. Figure 26 plots the net to gross ratios for the saturated zones of the Middle and

884 Lower Rio Rancho HSUs, depicted as bubble plots on a map of the study area. Figure 27 plots the net to
885 gross ratios for the saturated + unsaturated zone of the Middle Rio Rancho HSU. A net-to-gross value of
886 1.0 means all of the aquifer thickness is sand, and lesser values are the fractional value of sands out of a
887 total of 1.0. For example, a net-to-gross ratio of 0.2 means 20% sand.

888 Where both the MRR and LRR HSUs are penetrated by a well, the proportion of sand is greater in
889 the Lower Rio Rancho HSU compared to the Middle Rio Rancho HSU (Fig. 27). The averaged value of
890 sand gross-to-net ratios (Table 5) is greater in the Lower Rio Rancho HSU (0.52±0.20) compared to the
891 stratigraphically higher Middle Rio Rancho HSU (0.29±0.16) and Upper Rio Rancho HSU (0.34±0.24)
892 (errors correspond to one standard deviation; note the overlap between HSUs). HSU (but still within
893 error) compared to the two stratigraphically higher HSUs (0.52±0.20 vs. 0.34±0.24 and 0.29±0.16). This
894 is consistent with data presented above that show the Lower Rio Rancho HSU has greater sand
895 proportions than the Middle Rio Rancho HSU.

896 Within a given HSU there is an unexpected wide range of lateral variability, as illustrated in Table 5
897 and in the lithologic proportions of the Middle and Lower HSUs depicted in Figure 26-27. The Middle
898 RRU exhibits a coarsening upward trend in most wells, but the sand body ratios in the saturated zone
899 can differ by as much as 0.1-0.2 even for wells on the same fault-bounded block that lie within a couple
900 of kilometers distance from each other (e.g., Phoenix monitoring well vs. RRU-9; RRU-7 vs RRU-6A; RRU-
901 10 vs. RRU10A in Fig. 26). When one considers both the saturated and unsaturated zone for the Middle
902 Rio Rancho HSU, there is somewhat less variability between adjacent wells (cf. the MRR HSU data in
903 Figs. 26 and 27). This difference may be due to the saturated zone occupying different stratigraphic
904 levels in some adjacent wells, creating more variability in the net to gross ratios in Figure 26. But even
905 when both the saturated and unsaturated zones are considered (Fig. 26), there is generally not a
906 noteworthy south-southeastward fining trend over most of the study area (Fig. 27), parallel to the
907 paleoflow direction (paleoflow data from Connell, 2008a, 2008b; Koning et al., 1998; Cather et al., 1997;
908 Koning and Jochems, 2014; Koning and Rawlings, 2017). However, there is a suggestion (based on wells
909 RRU-9, RRU-23, RRU-18, RRU-15, PHX, and T1) that northward coarsening in the Middle Rio Rancho HSU
910 occurs from the approximate latitude of RRU-9 north to La Ceja. Perhaps that locale reflects the position
911 of paleofans, whereas downstream (to the south-southeast) the paleo depositional environment
912 approximated a gently sloping bajada or basin floor.

913 Density-porosity values were calculated for the saturated zones in each HSU per well in Kingdom
914 software from wireline data we digitized from sources listed in Appendix 1. Arithmetic means were

915 calculated for all strata in a HSU per well as well as for just the sand fraction, the latter delineated for
916 depth intervals where the Vshale ratio was 0.25 or less (Table 5). Although they lie within the 1-standard
917 deviation error range, these data suggest higher porosities for the Upper and Lower Rio Rancho HSUs
918 than the Middle Rio Rancho HSUs. When density-porosities are compiled for both the saturated +
919 unsaturated zones in a given well for only the sand bodies, the difference between the Upper and
920 Middle Rio Rancho HSUs is noteworthy (Fig. 28). We interpret this difference as reflecting less
921 compaction and less cementation of sand bodies in the Upper Rio Rancho HSU compared to the Middle
922 Rio Rancho HSU (e.g., Haneberg, 1995; Busch et al., 2022). Since the proportion of sand vs. clayey
923 sediment is only slightly higher in the Upper Rio Rancho HSU vs. the Middle Rio Rancho HSU, we infer
924 that the difference in porosity (due to compaction and cementation) may be a major factor why the
925 Upper Rio Rancho exhibits generally higher hydraulic conductivity values (Figs. 29-30, as discussed
926 below).

927

928 **Direct permeability analysis**

929 We used three approaches to measure vertical and lateral changes in permeability: compilation of
930 hydraulic conductivity and specific capacities from pumping tests, the Kozeny-Carman model, and the
931 Berg model. Note pumping-tests sample the saturated part of an entire screened interval in a given HSU,
932 whereas the Kozeny-Carman and Berg models calculates hydraulic conductivity as a function of depth in
933 a HSU per well.

934 Input information for the Kozeny-Carman and Berg models include sand grain sizes and effective
935 porosity. Sand grain sizes were obtained from sieve tests obtained during the drilling of the Rio Rancho
936 production wells (previously tabulated in consultant reports associated with a given well; Appendix 1).
937 We did not have empirical data giving effective porosity, so instead we substituted porosity measured
938 by the density-porosity tool in wireline logs (not available for all wells). Effective porosity represents the
939 connected pores in a sand that allow through-going water flow. Because the porosity measured by the
940 density-porosity tool is very likely higher than the effective porosity, **the permeability values we**
941 **obtained from these two models would theoretically be higher than the actual values**. **Thus, it is**
942 **important to note that we use the permeabilities from the Kozeny-Carman and Berg model only in a**
943 **comparative sense, that is, to compare lateral trends in permeability within a given hydrostratigraphic**
944 **unit.** Another potential problem with the Kozeny-Carman and Berg models is that the sand-size data

945 comes from a limited number of sieve analyses, consisting of 10-20 samples within a particular
946 hydrostratigraphic unit.

947 **Methods**

948 ***Pumping test hydraulic conductivity compilations per HSU***

949 We compiled hydraulic conductivity and specific capacity measurements from pumping tests (Table
950 6). These data were available for the Rio Rancho production wells (except RRU-18 and RRU-20), the
951 Bernalillo No. 4 well, and the three Intel production wells. Pump-test data were also available from the
952 extreme southwest of the study area and include the Black Ranch Test Hole and the Soil Amendment
953 Facility Well (BR and SAF-1 on Figure 29), the latter being 1 mile (1.6 km) south of the southern
954 boundary of the study area. Where more than one pump-test was conducted on a well, corresponding
955 to different depth-intervals of a particular HSU, the average of the hydraulic conductivities was used;
956 this was done for the Black Ranch test hole (BR), which had hydraulic conductivities of 12 ft/day and 5.4
957 ft/day in the Middle Rio Grande HSU, and in well RRU-13R, which had values of 1.2 and 0.8 ft/day in the
958 Middle Rio Grande HSU (Table 6). We selected the pumping tests for wells that had screened depths
959 that corresponded uniquely to a given HSU or were >80% within a given HSU. In the case of the Intel
960 wells, we attributed the pump test data as all being from the Upper Rio Rancho HSU, even though 20-
961 30% of the screens were in the Middle Rio Rancho HSU. This is because the Middle Rio Rancho HSU was
962 notably finer-grained than the Upper HSU, so we made the assumption that the pump test mostly
963 reflected the Upper Rio Rancho HSU. We could not use RRU-10A, RRU-12, RRU-16P, RRU-22, and NM
964 Util 4 wells because their screens extended significantly across multiple aquifers. Only one well, RRU-23,
965 had a pump test from a screened interval wholly within the Lower Rio Rancho aquifer.

966

Kozeny-Carman model

The Kozeny-Carman model calculates a theoretical hydraulic conductivity based on a referential grain size and effective porosity. It is based on a conceptual flow model that contained a bundle of capillary tubes of even length (Kozeny, 1927) that was later modified to account for tortuosity of flow around individual grains (Carman, 1937, 1939). The resulting equation is known as the Kozeny-Carman equation (equation 14 of Urumovic and Urumovic, 2016).

$$K = CF*[0.0625*D_g^2 *[(n_e^3/(1-n_e)^2]]$$

We assumed the effective porosity (n_e) is approximated by the porosities obtained by the density-porosity tool. Based on the results and recommendations of the paper by Urumovic and Urumovic (2016), we used the geometric mean of the sand grain size (D_g) derived from sieve analyses. We also use a correctional factor (CF) to account for temperature-based changes in water density and viscosity (CF = 0.7 + 0.03*Temperature of the groundwater in Celsius). The temperature of the groundwater was calculated from the local geothermal gradient and the depth of the sample. Local geothermal gradients were obtained mainly from plotting a regression line of bottom-hole temperature vs. bottom-hole depth data of the production wells. Near Well RRU-23, the geothermal gradient was calculated mostly using the temperature log for that well. Calculations were performed at one-foot depth intervals using Kingdom software; the one-foot depth calculations for a given HSU were then averaged to provide a representative value for a given HSU in a well (Table 6).

Berg model

The Berg model links effective porosity, grain size and grain sorting to permeability. Nelson (1994) interprets that it is a usable means of estimating permeability in unconsolidated to weakly consolidated sands (where porosity values are not much less than 30%) and clean, quartzose sandstone. The equation (3a of Berg, 1994) is:

$$k \text{ (in darcys)} = 5.1x10^{-6} * (\text{effective porosity in percent})^{5.1} * D^2 * e^{(-1.385p)}$$

The grain size input (D) is the median grain diameter, approximated by the 50th percentile in the sieve analyses. The porosity term (p) is the difference of the 90th percentile and 10th percentile in the sand-sieve analyses (expressed in phi units, where phi = -log$_2$ of the difference in these percentiles). Like in the Kozeny-Carman model, we assumed the effective porosity (n_e) is approximated by the porosities obtained by the density-porosity tool. Since the effective porosity is lower than the density-porosity values, the results over-estimate the true hydraulic conductivities. However, we used the results for comparative purposes, particularly in assessing if there is lateral variation in a given HSU.

Results

There are clear differences in the pump-test hydraulic conductivities and specific capacities for the Upper Rio Rancho versus Middle Rio Rancho HSUs. Hydraulic conductivities at a given well per HSU unit are depicted as bubble plots in Figure 29, where the width of the circle is scaled to the value of hydraulic conductivity. Note how the Upper Rio Rancho HSU data are notably larger than the Middle Rio Rancho HSU data. Both hydraulic conductivity and specific capacity data derived from pumping tests are shown in the box-and-whisker plots of Figure 30. For the Middle Rio Rancho unit, an outlier of 12 ft/day is plotted (from the Black Ranch test well, BR). For the Upper Rio Rancho unit, the median value is 9.25 ft/day and the first quartile (25 percentile) is 7 ft/day. The median value for the Middle Rio Rancho unit is 3.25 ft/day, whereas 75% of its values (up to the 75th percentile) lie at ≤ 5.35 ft/day, below the 25th percentile of the Upper Rio Rancho HSU (Fig. 30).

When standard deviations are plotted relative to the mean of data (pink lines in Fig. 30), one can see overlap between the Upper Rio Rancho HSU data within one standard deviation below the mean and the Middle Rio Rancho HSU data within one standard deviation above the mean. Similar overlap in the standard deviations of specific capacity and well production data presented in Riesterer et al. (2004) was used to justify there was no meaningful difference in permeability-related performance of wells screened in the Upper Rio Rancho HSU and those screened in the Middle Rio Rancho HSU. We acknowledge the overlap, but argue from our hydraulic conductivity data (Fig. 30) there is notably increased probability of encountering higher-permeabililty strata in the Upper Rio Rancho HSU compared to the Middle Rio Rancho HSU. Also, permeability-related data (including lithologic proxies)

plotted for individual wells strongly indicate more favorable permeability in the Upper Rio Rancho HSU compared to the Middle Rio Rancho HSU (e.g., Figs. 24 and 28).

Visual inspection of the map-plotted hydraulic conductivity data indicates that two wells in the southwest corner of the study area, returned relatively high hydraulic conductivities for the Middle Rio Rancho HSU (Fig. 29). In terms of geology, these higher results could possibly be due to increased input of medium-coarse sand into late Miocene paleo-drainage(s) as one goes southwestwards towards the mapped location of the Benavidez Member (exposures being located near the Rio Puerco). Such zones of coarser-grained sand were noted locally in the Arroyo Ojito Formation in the Black Range Test well (Appendix 3). The Benavidez member (spanning the Cerro Conejo and Arroyo Ojito Formations, Fig. 8) is a piedmont-slope deposit that transported relatively coarse-grained material off of the southeastern Colorado Plateau (Koning et al., 2021). It interfingers eastward with the Navajo Draw Member of the Arroyo Ojito Formation, is the latter being a fluvial deposit containing higher proportions of finer sand and mud (Connell et al., 1999; Koning and Jochems, 2014).

Compared to hydraulic conductivity data, there is more overlap when specific capacity data are presented as box and whisker plots (Table 2, Fig. 30). However, the Upper Rio Rancho HSU does exhibit a range of higher values than the Middle Rio Rancho HSU, with the higher 50% of data for the Upper Rio Rancho HSU being higher than the lower 75% of data for the Middle Rio Rancho HSU. Also, the median value of the specific capacity data is 10.5 gpm/ft for the Upper Rio Rancho HSU and 8.45 gpm/ft for the Middle Rio Rancho HSU.

Of the three studied HSUs, we only had enough data for the Middle Rio Rancho HSU to evaluate lateral permeability differences using the Kozeny-Carman and Berg models (Figures 31-32). As a reminder, these models calculate a theoretical hydraulic conductivity using sand-sieve analyses of 10-20 sand samples taken from cuttings at a given well. Using the sand sample depth-interval values (typically in increments of 10 ft), density-porosity values were extracted from a window centered on the corresponding depths from the wireline logs (e.g., ~5 ft on either side of the sample depth if the sampling interval was 10 ft). However, plotting the results of these analyses with hydraulic conductivities derived from pumping tests show very poor correlation, with R^2 values of <0.2 (Fig. 33a,b). Thus, we do not feel confident in using these particular data to make any interpretations regarding lateral permeability trends in the Middle Rio Rancho HSU. We explain this poor correlation by inferring: 1) the 10-20 sieve samples taken of the Middle Rio Rancho aquifer per well are insufficient in number to adequately characterize the this HSU, and/or 2) in actuality, because the sieve sample is not

1055 intact it does not adequately represent even the 10 ft-thick sampled interval because the drilling process
1056 homogenizes the sand and clayey beds and eradicates stratification-related controls of permeability .
1057 For example, it may be the case that a high-yielding sand bed is thinner than the 10 ft sieve-sample
1058 interval, and its unique properties are not adequately sampled. A higher number of samples or analyses
1059 of intact core would probably have yielded a better correlation with the pump test data.

1060 The only well log-associated parameter that seemed to somewhat correlate with pump test-derived
1061 hydraulic conductivities is the net-to-gross sand bodies, which had a R^2 of 0.56 (Figure 33c). "Net-to-
1062 gross" corresponds to the percentage of sand bodies in a given thickness interval – in our case, the
1063 thickness of a given hydrostratigraphic unit. This correlation of net-to-gross sand values with pump-test
1064 derived hydraulic conductivities allow us to use net-to-gross (percentage) of sand bodies as a proxy for
1065 relative permeability changes, which is useful in areas that lack pump-test data. Net-to-gross ratios of
1066 sand bodies are plotted in Figures 26-27.

1067 Assuming there is a correlation between higher net-to-gross values and overall permeability, the
1068 following vertical and lateral trends of net-to-gross values of sand bodies are noteworthy. First, where
1069 data from both the Middle and Lower Rio Rancho units are available in a single well, the net-to-gross
1070 values of the Lower Rio Rancho unit are greater than those of the Middle Rio Rancho HSU. In Figures 26
1071 and 27, one can see how yellow circles (representing the Middle Rio Rancho HSU) are smaller than the
1072 greener circles (representing the Lower Rio Rancho HSU). Second, for the Middle Rio Rancho HSU, net-
1073 to-gross values of sand bodies are variable across the study area, but there is a suggestion (based on six
1074 data points) that the northernmost part of the saturated Middle Rio Rancho HSU (may be slightly more
1075 permeable based on northward increasing sand body net-to-gross values. Specifically, the net-to-gross
1076 values for the saturated zone are 0.1-0.2 at wells RRU-9, RRU-23, and RRU-18, but those for wells >1 km
1077 to the north range from 0.2-0.7 (PHX, T1Y, RRU-15 wells in Table 5 and Fig. 26); this northward increase
1078 is present but more subtle in the map showing the net-to-gross values of both the saturated +
1079 unsaturated zone of the Middle Rio Rancho HSU (Fig. 27).

1080 In summary, tabulation of sands vs clays and the sand body net-to-gross data (Figs.23-24, 26-27)
1081 indicates that there is no strong lateral trend in sand proportion, which may be viewed as a proxy for
1082 permeability, to the north–northwest within the study area. Suggestions of coarsening to the NNW are
1083 most apparent outside of the Montoyas graben (Fig. 24). It is also ambiguous whether this trend exists
1084 in assessment of direct calculations of hydraulic conductivity using pump-test data (Fig. 29), possibly
1085 because of fewer wells used in the hydraulic conductivity compilation. Most of our analyses of lateral

permeability trends were conducted on the saturated part of the Middle Rio Rancho HSU. However, due to the sloping potentiometric surface (Fig. 11), variable well depths, and faulting within this HSU, the specific stratigraphic layers of the Middle Rio Rancho unit that are saturated vary from well to well and this might affect results. However, even when the unsaturated zone is taking into consideration in net to gross ratios (Fig. 27), there is still no obvious lateral trend. Based on these data, there is no incentive to prioritize future well drilling to the north-northwest due to possible lateral increases in permeability in that direction.

PRELIMINARY EVALUATION OF WATER QUALITY AND AGE

TDS Data

We compiled water quality data from water chemistry analyses of samples from Rio Rancho's wells, particular its main pumping wells (Appendix 1). Total dissolved solids (TDS) was chosen as an approximate proxy for overall water quality. Note that this simplistic exercise should be considered as only a preliminary investigation about the water quality and geochemistry of the northwestern Albuquerque basin, allowing comparison of updated knowledge of stratigraphy and structure (this report) with previous interpretations of Plummer (2004a,c).

The TDS data we compiled (Table 6) are plotted in Figure 34, where the Ziana horst is shaded in white. Note that the Coronado-Alameda fault delineates two TDS zones. To the southwest of the fault, TDS values are quite low, ranging from 205 to 462 ppm (Table 6), and are sampled from wells screened in either the Upper or Middle Rio Rancho HSUs. Within this western, low TDS zone, TDS values are slightly higher to the west of the Zia fault but overall quite acceptable (282-370 ppm per Table 6).

TDS values are higher on the northeast side of the Coronado-Alameda fault, corresponding to the Ziana horst, where they range from 388 to 1,400 ppm (Fig. 30; Table 6). Due to the northward pinch-out of the Upper Rio Rancho HSU, sampled aquifers in this area consist of the Middle and Lower Rio Rancho HSUs and the Zia HSU. A well along the Coronado-Alameda fault, RRU-16P, had moderately high values of 466 ppm.

Water samples east of the Ziana horst (i.e., east of the Tanaya fault), returned variable concentrations of TDS. Rio Rancho Utility 12 well, screened across both the Upper and Middle Rio Rancho HSUs and located 1 mile (1.6 km) east of the Tamaya fault and 0.3 miles (0.5 km) west of the san

Felipe fault, had TDS values of 461 ppm. Interestingly, well RRU-11, located 0.4 mi (0.6 km) east of the San Felipe fault and screened wholly within the Upper Rio Rancho HSU, had particularly high TDS values of 1,100 ppm. Unless there is surface-based contamination, the high TDS values for that well suggests the possibility of focused upwelling of relatively salty water along the nearby San Felipe fault.

Although considerably more work is needed to fully understand geologic influences on groundwater chemistry, these data indicate a spatial correspondence of saltier groundwater on and adjacent to the Ziana horst, particularly north of Northern Boulevard. Even the shallower aquifers in the northern part of the horst (such as the Middle RRU sampled in RRU-15, has relatively high TDS (530 ppm) compared to elsewhere in the study area.

Preliminary radiocarbon age analyses

We compiled data from previous radiocarbon age analyses that were conducted on groundwater in the northwestern Albuquerque basin (Plummer, 2004a,c). Radiocarbon ages are approximations of a groundwater age, being subject to complications due to dissolution of older carbon in calcium carbonate cements in the Santa Fe Group. Mixing of groundwater from different sources of different ages can also occur. Still, these ages can support or discredit hypotheses regarding groundwater flow paths and source areas, since younger ages should be present closer to recharge areas.

The radiocarbon data we compiled (Table 6) from ten wells are plotted in Figures 34–35, where the Ziana horst is shaded in transparent white. The youngest groundwater ages (4.5 to 14 ka) are associated with the Upper Rio Rancho HSU in the main part of the city of Rio Rancho (southern study area), south of the Coronado-Alameda fault. Groundwater ages from the Middle Rio Rancho HSU range from 13.5 to 28.5 ka. The younger half of these Middle Rio Rancho HSU ages (13.5-17.5 ka) are east of the Zia fault zone, where groundwater flow is southwestward or westward away from the Rio Grande towards the groundwater trough of Plummer et al. (2004a,c) in the south-central part of the study area(Fig. 35). The oldest groundwater ages come from west of the Zia fault zone, in wells RRU-9 and RRU-13 (20-28.5 ka). These data suggest relatively limited recharge to the Santa Fe Group aquifer west of the Zia fault zone.

DISCUSSION

Comparison with previous hydrochemical work

Work by Plummer (2004a,b,c) used a variety of geochemical data to map out various groundwater hydrochemical zones for the upper 2,000 ft of the Santa Fe Group aquifer system. The hydrochemical zones of interest to our study include the West-Central, Northwestern, Northern Mountain Front, and Central zones (west to east, shown in Fig. 11). The West-central zone has relatively moderate specific conductance and old radiocarbon groundwater ages; it is interpreted to have been recharged at relatively higher elevations and/or during a time of cooler climates. This water likely traveled southward to the western study area via long, deep flow paths sourced in the Jemez Mountains. We interpret that West-central zone water may discharge out of fractured bedrock along major faults that extend northwards towards the southern Jemez Mountains, such as the San Ysidro and Zia faults (Fig. 11). The West-central hydrochemical zone extends eastward under the adjoining Northwestern zone (see Plummer, 2004a,c). The Northwestern zone has relatively low specific conductance and likely recharged via low-elevation mountain-front recharge processes, with a component of infiltration from the Jemez River. Compared to the West-central zone, it is characterized by a zone of relatively shallow groundwater trending subparallel to the Jemez River. Likewise, the Northern Mountain front hydrochemical zone has relatively dilute water (low specific conductance) and recharged from the southern margin of the Jemez Mountains, with some infiltration occurring along the Rio Grande. The Central hydrochemical zone is centered on the Rio Grande. Chemical constituent and isotope (^{14}C, ^{2}H) data indicate Rio Grande infiltration provides the primary source of recharge for the Central zone.

The presence of a long-term groundwater "trough" coinciding with the southern Montoyas graben was noted by Bexfield and Anderholm (2000) and Plummer et al. (2004a,c). This trough is marked by the water table surface being relatively low, about 100 ft lower than near the Rio Grande. Plummer (2004a) view this trough as a transient feature perhaps reflecting lower rates of recharge from the Rio Grande during the drier middle-late Holocene; prior to that time the water-table surface may have been about the same elevation (in a west-east direction). The transitory nature is inferred by the reasoning that a long-term trough would result in the groundwater there (corresponding largely to the West-central zone) having much more chemical affinity with the Rio Grande (Central Zone), since a long-term water-table gradient would presumably drive Rio Grande flow towards that trough.

We emphasize that the groundwater trough coincides with geologic structures, particularly its alignment with the southern Montoyas graben, and that faults bounding this graben may be acting as groundwater barriers. Such a barrier effect is manifested by the geometry of the cones of depressions associated with two areas: RRU-9 and the closely spaced NMU-1 and W-4 wells. In particular, these

cones of depressions appear to be elongated north-south, parallel to nearby major faults (e.g., San Ysidro, Zia, Dovall faults; Figs. 11, 35). The high water-table gradients parallel to the northern Coronado-Alameda fault and the east-west faults near RRU-10 are consistent with those faults acting as groundwater barriers. We also note that the water-table geometry in southeast Rio Rancho very likely indicates a major component of recharge from the Rio Grande, accounting for the young C-14 ages in that area (e.g., wells RRU-2 and the Intel production well 2; Table 6). However, westward flow further west may be hampered by north-south structures, like the inferred fault along Universe Boulevard, or perhaps subsurface basaltic dikes. This retarded flow may result in the recharge rate of relatively young groundwater (from the Rio Grande) being comparable, or perhaps less than, the deep-recharge replenishing the West-central zone. The result would be a blended water that still retains much of the chemical character of the West-central zone. Further modeling work could be used to test this alternative hypothesis regarding groundwater flow and groundwater chemistry near the southern end of the groundwater trough in our study area.

We suggest a spatial conceptualization of the hydrogeology as "regimes" by synthesizing both groundwater flow, hydrochemical zones, and geologic structure (Fig. 35). These hydrogeologic regimes generally follow the hydrochemical zones of Plummer et al. (2004a,c) but we add the Ziana regime corresponding to most of the Ziana horst. We infer that the eastern boundary of the West-central zone is strongly controlled by various north-south faults that act as fault barriers to some degree. These faults likely include the central Zia fault, the middle Doval fault, and the fault paralleling Universe Boulevard. These faults allow some mixing of water from the northeast and east in the southern part of the trough shown in Figure 35. But old-groundwater in the northern part of the trough, in the West-central regime, is largely a product of subsurface discharge along the San Ysidro and perhaps Zia faults. These faults transfer groundwater (probably in fractured bedrock) southwards to the study area from the Jemez Mountains. Compared to the Northwestern regime to the west and the Northern Mountain Front regime to the east, the Ziana regime is heavily influenced by salty (high TDS) water discharging from elevated, fractured and faulted bedrock. The western boundary of the Central hydrogeologic regime is extended westward in the southeastern corner of the study area based on groundwater elevation contours. This groundwater is interpreted to be largely derived from the Rio Grande (Plummer et al., 2004a,c), consistent with low TDS values and low radiocarbon ages (Figs. 34–35). A leaky fault barrier is inferred to allow minor groundwater flow from the Central zone to the West- central zone, but this flow is insufficient to notably alter the geochemical signature of the West-central zone.

Interpretations relevant for groundwater management

1. The Upper Rio Rancho HSU is the most favorable of the HSUs

Although there is some overlap in hydraulic conductivity data between the Upper and Middle Rio Rancho HSUs, the upper range of hydraulic conductivity data in the Upper Rio Rancho HSU include considerably higher values and its median value is 3 times greater than the median value of the Middle Rio Rancho HSU. (Figs. 29-30; Table 6). The Upper Rio Rancho HSU also exhibits the lowest TDS groundwater (Fig. 34), excluding the anomalous data at well RRU-11, and is the shallowest HSU. Therefore, the Upper Rio Rancho HSU can be considered as the most favorable HSU for groundwater extraction potential. However, most of the Upper Rio Rancho HSU is unsaturated, with its saturated area being located in the southeastern corner of the study area and along the eastern boundary (Figs. 15, 18).

The extent and thickness variations of the saturated portion of the Upper Rio Rancho HSU is shown in Figure 18. The saturated-Upper Rio Rancho HSU thickens to the southeast, towards the intersection of Coors and Paseo del North (partly due to the increase in the elevation of the potentiometric surface in that direction), and thins to the north. It may possibly thin abruptly, by perhaps ~1,000 ft (~300 m), westward across the inferred east-down fault near Universe Boulevard, but more data is needed to ascertain the magnitude and rate of this thinning. Near the western extent of Paseo del Norte, extending north to southern Boulevard, the saturated Upper Rio Rancho is <500 ft (<150 m) thick, thinning in this zone to the west and north. It does not extend west of the Zia fault. The north edge of the saturated Upper Rio Rancho HSU lies between Southern and Northern boulevards, and it thins abruptly northeast of the Coronado fault. East of the Tamaya fault in the northeastern study area, the saturated Upper Rio Rancho HSU is inferred to be several hundred feet thick, thickening even more (>1,000 ft, >300 m) east of the Santa Ana section of the San Felipe fault.

2. The eastern and southeastern parts of study area have favorable hydrogeology

Where the saturated Upper Rio Rancho HSU is thickest mainly corresponds with the Central and Northern Mountain hydrogeologic regimes. TDS values are low in these areas, except locally near faults (e.g., RRU-12). Young (<15,000 year) radiocarbon ages and groundwater flow directed away from rivers suggests a component of recharge from relatively young surface waters (Fig. 35). In terms of hydrogeologic properties, this area may be viewed as favorable for groundwater extraction potential.

3. The saturated Middle Rio Rancho HSU is important because of its large extent and thickness

The extent and thickness variations of the saturated portion of the Middle Rio Rancho HSU is shown in Figure 19. Note that it extends notably further northwest compared to the Upper Rio Rancho HSU, reaching to the San Ysidro fault. West of the Zia fault and north of Southern Boulevard, its saturated thickness is 1,000-1,500 ft (300-460 m), increasing southward to 2,000 to 2,500 ft (610-760 m) within 2 miles west of the west end of Paseo del Norte. A 1,200-3,000 ft-thick (365-910 m-thick) prong of saturated Middle Rio Rancho HSU extends northward into the Montoyas graben, inferred as being thickest between the Zia and Doval faults and thinning eastward from the Doval fault. The saturated part of the Middle HSU covers much more of the Ziana horst than the saturated-Upper Rio Rancho HSU, pinching out northward near RRU-23 and the northern end of Unser Boulevard. The saturated-Middle Rio Rancho unit is >1,500 ft (>460 m) thick east of the Tamaya fault, and is inferred to be >2,000 ft (>600 m) east of the Santa Ana section of the Felipe fault. In the southeast corner of the study area, the saturated Middle Rio Rancho HSU is interpreted to be 2800–4400 ft (850–1340 m; Fig. 19).

Our sand vs. clay permeability proxies, obtained from well data, suggests that the Middle Rio Rancho HSU has generally lower permeabilities at a given site compared to the Lower and Upper Rio Rancho HSUs (Figs. 25–28). This is confirmed by the compilation of hydraulic conductivities and specific capacities obtained from pumping tests (Figs. 29-30), although these also show considerable overlap in the data. However, the relatively high, aforementioned thickness of the Middle Rio Rancho HSU would result in relatively high transmissivities (T = hydraulic conductivity times thickness of saturated sediment), and the TDS values compiled for this unit were <500 ppm west and southwest of the Ziana horst. Therefore, one can consider the Middle Rio Rancho HSU as an important component in groundwater management for the northwestern Albuquerque basin.

Except for possibly two areas, we do not find any notable lateral permeability trends over most of the study area for the Middle Rio Rancho HSU (Fig.27-29). The first of the two exceptions is located in the northwestern corner of the city's municipal boundary. Based on relatively higher sand body proportions in the Phoenix monitoring, the Tamara #1-Y, and the RRU-15 wells compared to wells to the south (Figs. 23, 26-27), there may be a slight northward coarsening of the Middle Rio Rancho HSU, and corresponding increase in permeability at distances >4 miles (6 km) north of Northern Boulevard.

The second area is in the southwestern corner of the current boundary of the Rio Rancho municipality. There, pumping test data indicate hydraulic conductivities of 5-12 ft/day (Fig. 29; Table 6), which is more than the values of 2-5 ft/day plotted closer to the main, urbanized part of Rio Rancho (Fig. 29). The increased hydraulic conductivities there may be due to tongues of the relatively coarse-grained

Benavidez Member (Koning et al., 2021), which are observed in exposures west of the Ceja del Rio Puerco and whose tongues may extend into the Arroyo Ojito Formation (Middle Rio Ranch HSU) in the Black Ranch test well (depths of 840-1010, 2490-2540, 2710-2740, and 2890-2900 ft, Appendix 3).

4. Inferred groundwater extraction limitations in Middle and Upper Rio Rancho HSUs to west

West of the longitude corresponding to Universe Boulevard, west of 106° 45'0"), there are a number of issues that may limit groundwater extraction. One, the Upper Rio Rancho HSU, which we interpret as a relatively high-permeability HSU, is thin west of Universe and south of Southern Boulevard; here, it is less than 600 ft and thins to the northwest. Two, the groundwater table is particularly low in this area, corresponding to a temporally persistent trough (Anderholm and Bexfield, 2000). Groundwater radiocarbon ages are also old (15,000-29,000 years). This area corresponds to the West-central hydrochemical zone of Plummer (2004a,c), where recharge is inferred to be ultimately derived from higher elevations in the Jemez Mountains (and/or in cooler temperatures) and probably discharged from faulted bedrock at the base of the Santa Fe Group. The fact that the upper bedrock consists of Mesozoic–upper Paleozoic strata (Koning et al., 2014; Koning and Rawling, 2017) makes it difficult to reconcile with low TDS values of the groundwater (e.g., deep aquifers drilled in these strata return high TDS waters; e.g., Intera, 2008), which lends credence to the hypothesis of local recharge during an ice age. Although groundwater quality is relatively favorable, notable drawdown in two areas (RRU-9 and NMU-1 + W-4) strongly suggest permeability is poor and recharge is limited. Other data suggesting low permeabilities is the lithologic proportion of sand (Figs. 23, 25–27) and pumping test data in the Middle Rio Rancho HSU (Figs. 29-30). An apparent exception is in the southwest part of the study area, where two pumping tests show relatively higher hydraulic conductivities (Soil Ammendment Facility well and Black Ranch well). North of Southern Boulevard and west of the City's municipal boundary, a conservative approach in groundwater extraction would be prudent based on available data.

5. The Ziana horst – a problem and possibly an opportunity

The middle and northern part of the Ziana horst, particularly north of Northern Boulevard, is spatially associated with high TDS and poorer quality groundwater (Figs. 34-35). These issues are exemplified by the groundwater quality problems (Riesterer and Drakos, 2008) and lack of current pumping at well RRU-23. The Ziana horst corresponds to our informal Ziana hydrogeologic regime, where groundwater flow is southwards and TDS is relatively high (Fig. 35). The salty water is probably a result of upwelling of deep water from the relatively high (structurally elevated), faulted (and presumably fractured at depth) horst block. Deep-water flow may also be directed southwards in the

lower Zia HSU between north-striking faults from the Jemez Mountains. Future water-well drilling in this zone probably has the best chances for success to the south, since the Upper and Middle Rio Rancho HSUs thicken southward and the (Figs. 18–19) and TDS values also lessen in that direction (Fig. 35).

A potential opportunity for groundwater management is the documentation of a 1,280 ft- (390 m-) thick, sandy zone in the lower-middle Zia HSU (Fig. 36). Based on outcrop correlatives of this zone near La Ceja and Ceja del Rio Puerco, corresponding to the Piedra Parada Member of the Zia Formation, there is localized cementation of this unit (at least in that location) but moderate to strong cement is typically <15-20% of the Member's volume (approximate visual estimate). If this low amount of cementation extends to the Ziana horst, then the lower-middle Zia HSU may be relatively permeable and a target aquifer. But water from such an aquifer would need to be subjected to desalinization or blending to achieve water quality standards, and whether such treatment or blending is practical or economically feasible warrants further study.

6. `The Lower Rio Rancho HSU: probably high permeability but poor water quality

Sand-body thicknesses and the proportion of sand (net vs. gross ratios) indicate that the Lower Rio Rancho should have relatively high permeabilities (Figs. 26-27). This inference is bolstered by the single pumping test of this unit (RRU-23), which returned a notably high value of 21 ft/day (Fig. 30). Being observed in RRU-13R as well as on the Ziana horst, we interpret that this higher-permeability unit extends across the northern two-thirds of the study area. However, the apparent absence of this unit in the Black Ranch test well suggests a possible facies change to a finer-grained unit south of Southern Boulevard (Plate 3). Furthermore, there may be higher TDS values seen in wells sampled in this unit, particularly on the Ziana horst, compared to wells sampled in the Middle Rio Rancho HSU and the Upper Rio Rancho HSU.

Stratigraphic and tectonic findings

The work involved in correlating stratigraphic units in the subsurface across the study area, aided by Kingdom software analysis, resulted in the following observations pertaining to Santa Fe Group stratigraphy and Rio Grande rift tectonics.

- In southward direction, it is increasingly difficult to differentiate the Loma Barbon vs. Navajo Draw Members of the Arroyo Ojito Formation. This differentiation becomes particularly difficult

south of Northern Boulevard. This is probably due to southward converging of the two paleo-drainage systems and back-and-forth, east-west shifting of the common boundary.

- The Lower Rio Rancho HSU is extensive in an east-west direction, and does not appear to thin across the Ziana horst block; rather, eastward thickening may occur in that direction, consistent with NE-thickening of the Cerro Conejo Formation in the cross sections in Riesterer et al. (2008). But this coarse-grained unit may grade southward into a finer-grained facies in southern part of study area, particularly south of Southern Boulevard. During its deposition ca. 13–10 Ma, the Lower Rio Rancho HSU appears to reflect a wide, south-southeast-flowing distributary fan complex with relatively high stream power that carried copious sand eroded from the southeastern Colorado Plateau. Sand ablated from this fluvial system likely formed the Ojo Caliente sand dune field to the northeast, based on the same age of that dune field (cf. Connell, 2008a, and Koning et al., 2011) to the Lower Rio Rancho HSU (upper Cerro Conejo Formation), the down-wind position of that dune filed (based on paleo-wind measurements of the Ojo Caliente sandstone; e.g., Koning et al., 2003, 2005; Koning, 2003), and broadly similar sand composition.
- Two observations indicate that the Ziana horst was notably tectonically active after ~11 Ma. First, the LRR either thickens eastward or maintains about the same thickness across the Ziana horst, but the overlying Middle and Upper Rio Rancho HSUs thin across this structure (Plates 5-7; Figs. 18-19
- Second, 11.2-11.3 Ma Trapper Creek B ashes are seen on the ground surface on the footwall of the Arroyo Venada fault, one of the major eastern-bounding faults of the horst, but lie at 2,070-2,080 ft depth on the hanging wall of the fault (in well RRU-18). Based on our structural contour map (Plate 3), there is ~500–1000 ft of post-10 Ma east-down vertical offseton that fault of the ca. 10 Ma upper contact of the Lower Rio Rancho HSU(Appendix 7; age data from Connell et al., 1999; Connell, 2008b). Elsewhere, there is 1,400 ft (430 m) of throw of this contact by the Zia fault in the northern study area, and facies changes are observed in the Navajo Draw Member immediately adjacent to Zia fault (on its hanging wall; see Koning and Personius, 2002). The top of the Middle Rio Rancho HSU, corresponding to ~6 Ma (Fig. 6, Connell, 2008b), is offset ~200 ft (~60 m) on the northern Zia fault. Therefore, much fault activity occurred in this part of the study area in the late Miocene through the Pliocene, with the highest rates of throw between 10 and 6 Ma. However, the Ziana horst and adjoining fault also may have been active in the late

Oligocene-early Miocene, based on lithostratigraphic analyses of oil test holes drilled in the study area (Connell et al., 2007).

CONCLUSION

Our study differentiated four hydrostratigraphic units (HSUs) in the northwestern Albuquerque basin, mapped them in the subsurface, and assessed permeability differences between and within them. We constructed a 3D, geologic model showing the elevations of the bounding surfaces of these HSUs, and this model explicitly includes major faults that offset them. This model will be essential for potential future studies for calculating groundwater volumes and for creating groundwater-flow models of the area. Although there is overlap in the data, the Upper Rio Rancho HSU exhibits a higher hydraulic conductivity values (compiled from pumping tests) compared to the Middle Rio Rancho HSU, consistent with its higher sand/clay ratio inferred from well data and its higher density-porosity values. Furthermore, the TDS values of the Upper Rio Rancho HSU are quite acceptable, typically being 200-400 ppm. However, the thick saturated portions of the Upper Rio Rancho HSU are only found east of the Tamaya fault and in the southeastern part of the study area, south of Southern Boulevard and south of the Coronado-Alameda fault. The saturated Middle Rio Rancho HSU is over 1,000 ft thick across most of the study area, including a northward prong extending upward between the Ziana horst and the Zia fault. Several wells indicate a coarsening upward trend in this HSU (e.g., Fig. 12), so areas where its upper part is saturated are more favorable than where just its lower part is saturated. There are no strong lateral permeability trends across the saturated portion of the Middle Rio Rancho HSU over most of the study area, but hydraulic conductivities compiled from pumping tests do indicate higher permeability values in the southwest part of the study area, within 5 miles (8 km) northwest of the western end of Paseo del Norte. A northward increase in sand proportions also occurs north of the approximate latitude of RRU-9 (35°20’0”), suggesting a possible increase in permeability that remains to be confirmed by pumping-test data. The Lower Rio Rancho HSU commonly exhibits relatively high TDS values, but various well-based permeability proxies and a single pumping test, in agreement with field observation of a high sand content, indicates it has relatively high permeability. The Lower Rio Rancho HSU extends across the northern 2/3 of the study area, but may possibly undergo a southward facies change to a finer-grained unit south of Southern Boulevard. The lower-middle Zia HSU is notably sandy, based on outcrop observations and wildcat oil well data. Its relatively higher elevation on the Ziana horst may possibly provide an accessible deep-water aquifer in that area, given that economically feasible

methods can be found to either treat the high salinity or blend its groundwater to meet acceptable standards. An ancillary result of our study is a refinement of interpretations of past rift activity. Comparison of the amount of displacement of various-aged HSU surfaces across certain faults, in addition to stratigraphic positions of unconformities, indicates that notable tectonic activity associated with the Ziana horst and bounding faults occurred in the late Miocene. Motion along the east-down Zia fault to the west was particularly high in the middle and late Miocene, and throw rates decreased in the Plio-Pleistocene.

REFERENCES

Aigner, T., Asprion, U., Hornung, J., Junghans, W.-D., and Kostrewa, R., 1996, Integrated outcrop analogue studies for Triassic alluvial reservoirs: examples from southern Germany: Journal of Petroleum Geology, v. 19, issue 4, p. 393–406.

Al-Ajmi, H., Hinderer, M., Kller, M., Rausch, R., Blum, P., and Bohnsack, D., 2011, The role of outcrop analogue studies for the characterization of aquifer properties: International Journal of Water Resources and Arid Environments: v. 1, no 1, p. 48-54.

Allen, B.D., Connell, S.D., Hawley, J.W., and Stone, B.D., 1998, Core drilling provides information about Santa Fe Group aquifer system beneath Albuquerque's west side: New Mexico Geology, v. 20, n. 1, p. 9-13.

Bartolino, J.R., and Cole, J.C., 2002, Ground-water resources of the Middle Rio Grande Basin, New Mexico: U.S. Geological Survey Circular 1222, 132 p.

Becker, I., Busch, B., Koehrer, B., Adelmann, D., Hilgers, C., 2019, Reservoir quality evolution of upper Carboniferous (Westphalian) tight gas sandstones, lower Saxony basin, NW Germany, Journal of Petroleium Geology, v. 42, no. 4, p. 371-392.

Bexfield, L.M., and Anderholm, S.K., 2000, Predevelopment water-level map of the Santa Fe Group aquifer system in the Middle Rio Grande Basin between Cochiti Lake and San Acacia, New Mexico: U.S. Geological Survey Water—Resources Investigations Report 00-4249, 1 sheet.

Bexfield, L.M., and Anderholm., S.K., 2002, Estimated water-level declines in the Santa Fe Group aquifer system in the Albuquerque area, central New Mexico, predevelopment to 2002: U.S. Geological Survey Water—Resources Investigations Report 02-4233, 1 sheet.

Bexfield, L.M., and Plummer, L.N., 2003, Occurrence of arsenic in ground water of the Middle Rio Grande Basin, central New Mexico; in Welch, A.H., and Stollenwerk, K.G., eds., Arsenic in Ground Water: Geochemistry and Occurrence, Kluwer Academic Publishers, Chapter 11, p. 295-327.

Bexfield, L.M., Lindberg, W.E., and Anderholm, S.K., 1999, Summary of water-quality data for City of Albuquerque drinking-water supply wells, 1988-97: U.S. Geological Survey, Open-file Report 99-195, 138 p., 1 pl.

Bexfield, L.M., Danskin, W.R., McAda, D. P., 2004, Simulation-optimization approach to management of ground-water resources in the Albuquerque area, New Mexico, 2006 through 2040: U.S. Geological Survey, Scientific Investigations Report 2004-5140, 82 p.

Biteman, S.E., Hyndman, D.W., Phanikumar, M.S., and Weissmann, G.S., 2004, Integration of sedimentologic properties for improved transport simulations, *in* Bridge, J.S., and Hyndman, D.W., eds., Aquifer characterization: SEPm Special Publication No. 80, p. 3–13.

Black, B.A., and Hiss, W.L., 1974, Structure and stratigraphy in the vicinity of the Shell Oil Co. Santa Fe Pacific No. 1 Test Well, southern Sandoval County, New Mexico, *in* Siemers, C.T., Woodward, L.A., and Callander, J.F., eds., Ghost Ranch: New Mexico Geological Society, 25th Annual Fall Field Conference Guidebook, p. 365-370.

Brandes, N.N., 2002, Lithostratigraphy and petrography of upper Santa Fe Group deposits in the northern Albuquerque Basin, New Mexico [M.S. thesis]: Socorro, New Mexico Institute of Mining and Technology, 208 p.

Bryan, K., and McCann, F.T., 1937, The Ceja de l Rio Puerco: A border feature of the Basin and Range province in New Mexico. I. Stratigraphy and Structure: Journal of Geology, v. 45, p. 801-828.

Bryan, K., and McCann, F.T., 1938, The Ceja del Rio Puerco: A border feature of the Basin and Range province in New Mexico. II. Geomorphology: Journal of Geology, v. 46, p. 1-16.

Busch, B., Spitzner, A-D, Adelmann, D., and Hilgers, C., 2022, The significance of outcrop analog data for reservoir quality assessment: A comparative case study of Lower Triassic Buntsandstein sandstones in the Upper Rhine Graben: Marine and Petroleum Geology, v. 141, 17 p.

Caine, J.S., and Minor, S.A., 2009, Structural and geochemical characteristics of faulted sediments and inferences on the role of water in deformation, Rio Grande rift, New Mexico: Bulletin of the Geological Society of America: v. 121, nos. 9–10, p. 1325–1340.

Carman, P.C., 1937, Fluid flow through granular beds: Transactions, Institution of Chemical Engineers, v. 15, p. 150–166.

Carman, P.C., 1939, Permeability of saturated sands, soils, and clays: The Journal of Agricultural Science, v. 29, no. 2, p. 262–273.

Cather, S.M., Connell, S.D., Heynekamp, M.R., and Goodwin, L.B., 1997, Geology of the Arroyo de las Calabacillas (Sky Village SE) 7.5-minute quadrangle, Sandoval County, New Mexico: New Mexico Bureau of Mines and Mineral Resources, Open-file Geologic Map 9, scale 1:24,000.

Chapin, C.E., and Cather, S.M., 1994, Tectonic setting of the axial basins of the northern and central Rio Grande rift, *in* Keller, G.R., and Cather, S.M., eds., Basins of the Rio Grande Rift: Structure, Stratigraphy, and Tectonic Setting: Boulder, Colorado, Geological Society of America Special Paper 291, p. 5-25.

Cikoski, C.T., Koning, D.J., and Connell, S.D., 2012, Geologic map of the La Mesita Negra quadrangle: New Mexico Bureau of Geology and Mineral Resources, Open-file Geologic Map 223, scale 1:24,000.

Connell, S.D., 1997, revised Feb of 2000, Geology of the Alameda quadrangle, Bernalillo and Sandoval Counties, New Mexico: New Mexico Bureau of Mines and Mineral Resources, Open-file Geologic Map 10, scale 1:24,000.

Connell, S.D., 2004, Geology of the Albuquerque Basin and tectonic development of the Rio Grande rift, north-central New Mexico, in Mack, G.H., and Giles, K.J., eds., The Geology of New Mexico, A geologic history: New Mexico: New Mexico Geological Society, Special Publication 11, p. 359-388.

Connell, S.D., 2006, Preliminary geologic map of the Albuquerque-Rio Rancho metropolitan area and vicinity, Bernalillo and Sandoval Counties, New Mexico: New Mexico Bureau of Geology and Mineral Resources, Open-file Report 496, 1:50,000

Connell, S.D., 2008a, Geologic map of the Albuquerque-Rio Rancho metropolitan area and vicinity, Bernalillo and Sandoval Counties, New Mexico: New Mexico Bureau of Geology and Mineral Resources, Geologic Map 78, 1:50,000

Connell, S.D., 2008b, Refinements to the stratigraphic nomenclature of the Santa Fe Group, northwestern Albuquerque basin, New Mexico: New Mexico Geology, v. 30, n. 1, p. 14-35.

Connell, S.D., Allen, B.D., and Hawley, J.W., 1998, Subsurface stratigraphy of the Santa Fe Group using borehole geophysical logs, Albuquerque area, central New Mexico: New Mexico Geology, v. 20, n. 1, p. 2-7.

Connell, S.D., Koning, D.J., and Cather, S.M., 1999, Revisions to the stratigraphic nomenclature of the Santa Fe Group, northwestern Albuquerque Basin, New Mexico; in Pazzaglia, F.J., and Lucas, S.G., eds., Albuquerque Geology: New Mexico Geological Society, Guidebook 50, p. 337-353.

Connell, S.D., Koning, D.J., and Derrick, N.N., 2001, Preliminary interpretation of Cenozoic strata in the Tamara No. 1-Y well, Sandoval County, north-central New Mexico; in Connell, S.D., Lucas, S.G., and Love, D.W., eds., Stratigraphy and tectonic development of the Albuquerque Basin, central Rio Grande rift, mini-papers for field trip guidebook: Albuquerque, New Mexico: Geological Society of America, Rocky Mountain-South Central Section Meeting: New Mexico Bureau of Geology and Mineral Resources, Open-file report 454B, p. K79-K88.

Connell, S.D., Koning, D.J., Kelley, S.A., and Brandes, N.N., 2007, Oligocene-Miocene sedimentation in the southwestern Jemez Mountains and northwestern Albuquerque basin, New Mexico; in Kues, B.S., Kelley, S.A., and Lueth, V.W., eds., Geology of the Jemez Region II: New Mexico Geological Society, Guidebook 58. p. 195-208.

Connell, S.D., Smith, G.A., Geissman, J.W., and McIntosh, W.C., 2013, Climatic controls on nonmarine depositional sequences in the Albuquerque Basin, Rio Grande rift, north-central New Mexico, *in* Hudson, M.R., and Grauch, V.J.S., eds., New Perspectives on Rio Grande Rift Basins: From Tectonics to Groundwater: Geological Society of America Special Paper 494, p. 383-425, doi: 10.1130/2013.2494(15).

Davis, J.M., Lohmann, R.C., Phillips, F.M., Wilson, J.L., Love, D.W., 1993, Architecture of the Sierra Ladrones Formation, Central New Mexico: depositional controls on the permeability correlation structure: Geological Society of America Bulletin, v. 105, p. 998–1007.

Fetter, C.W., Jr., 2018, Applied Hydrogeology: Long Grove, Illinois, Waveland Press, chapter 3.

Galanter, A.E., and Curry, L.T.S., 2019, Estimated 2016 groundwater level and drawdown from predevelopment to 2016 in the Santa Fe Group aquifer system in the Albuquerque area, central New Mexico: U.S. Geological Survey Scientific Investigations Map 3433, 1 sheet, 13-p. pamphlet, https://doi.org/10.3133/sim3433.

Galusha, T., 1966, The Zia Formation, new early to medial Miocene beds in New Mexico: American Museum Novitates, no. 2271, p. 1-12.

Gawne, C., 1981, Sedimentology and stratigraphy of the Miocene Zia Sand of New Mexico, summary: Geological Society of America, Bulletin, Part I, v. 92, no. 12, p. 999-1007.

1509 Gaud, M.N., Smith, G.A., and McKenna, S.A., 2004, Relating small-scale permeability heterogeneity to
1510 lithofacies distribution, *in* Bridge, J.S., and Hyndman, D.W., eds., Aquifer characterization: SEPm
1511 Special Publication No. 80, p. 56–66.

1512 Gillentine, J.M., 1994, Petrology and diagenesis of the middle and lower Santa Fe Group in the northern
1513 Albuquerque Basin, New Mexico: New Mexico Bureau of Mines and Mineral Resources, Open-file
1514 report 402C, Chapter 6, p. 1-50, 4 app.

1515 Grauch, V.J.S., 1999, Principal features of high-resolution aeromagnetic data collected near
1516 Albuquerque, New Mexico: New Mexico Geological Society, Guidebook 50, p. 115-118.

1517 Grauch, V.J.S., Keller, G.R., and Gillespie, C.L., 1999, Discussion of new gravity maps for the Albuquerque
1518 Basin area: New Mexico Geological Society, Guidebook 50, 119-124.

1519 Grauch, V.J.S., Hudson, M.R., Minor, S.A., 2001, Aeromagnetic expression of faults that offset basin fill,
1520 Albuquerque Basin, New Mexico: Geophysics, v. 66, n. 3, p. 707-720.

1521 Grauch, V.J.S., and Connell, S.D., 2013, New perspectives on the geometry of the Albuquerque Basin, Rio
1522 Grande rift, New Mexico: Insights from geophysical models of rift-fill thickness, *in* Hudson, M.R., and
1523 Grauch, V.J.S., eds., New Perspectives on Rio Grande Rift Basins: From Tectonics to Groundwater:
1524 Geological Society of America Special Paper 494, p. 427-462, doi: 10.1130/2013.2494(16).

1525 Haneberg, W.C., 1995, Compaction curves and virgin specific storage estimates for selected
1526 Albuquerque basin water wells, *in* Haneberg, W.C., and Hawley, J.W., eds., Characterization of
1527 hydrogeologic units in the northern Albuquerque Basin: New Mexico Bureau of Mines and Mineral
1528 Resources Open-file Report 402-C, p. 4-1 to 4-31.

1529 Hornung, J., and Aigner, T., 2006, Reservoir architecture in a terminal alluvial plain: an outcrop analogue
1530 study (Upper Triassic, southern Germany) Part 1: Sedimentology and petrophysics: Journal of
1531 Petroleum Geology, v. 25, issue 1, p. 3–30.

1532 Howell, J.A., Martinius, A.W., Good, T.R., 2014, The application of outcrop analogues in geological
1533 modelling: a review, present status, and future outlook: Geological Society of London Special
1534 Publication 387 (1), p. 1-25. https://doi.org/10.1144/sp387.12

Hawley, J.W., 1996, Hydrogeologic framework of potential recharge areas in the Albuquerque Basin, central New Mexico: New Mexico Bureau of Mines and Mineral Resources, Open-file report 402 D, Chapter 1, 68 p.

Hawley, J.W., and Haase, C.S., 1992, Hydrogeologic framework of the northern Albuquerque Basin: New Mexico Bureau of Mines and Mineral Resources, Open-file Report 387.

Hawley, J.W., Haase, C.S., Lozinsky, R.P., 1995, An underground view of the Albuquerque Basin: New Mexico Water Resources Research Institute, Report 290, p. 27-55.

Intera Inc., 2008, Sandoval County Rio Puerco Basin Water Development Project, Aquifer Test and Analysis Report: unpublished consultant report prepared for Sandoval County (Dec 9, 2008), 46 p. and Appendices A–E.

Keller, M., Bohnsack, D., Koch, R., Hinderer, M., Hornung, J., Al-Ajmi, H., and Amarah, B.A., 2019, Outcrop analog studies of the Wasia-Biyadh and Aruma aquifers of Saudi Arabia, in AlAnzi, H.R., Rahmani, R.A., Steel, R.J., and Soliman, O.M., eds., Siliclastic reservors of the Arabian Plate: The American Association of Petroleum Geologists, v. 116, https://doi.org/10.1306/13642171M1183514

Kelly, V.C., 1977, Geology of the Albuquerque Basin, New Mexico: New Mexico Bureau of Mines and Mineral Resources, Memoir 33, 60 p.

Kernodle, J.M., 1998, Simulation of ground-water flow in the Albuquerque Basin, central New Mexico, 1901-95, with projections to 2020: U.S. Geological Survey Open-File Report 96-209, 54 p.

Kernodle, J.M., and Scott, W.B., 1986, Three-dimensional model simulation of steady-state ground-water flow in the Albuquerque-Belen Basin, New Mexico: U.S. Geological Survey Water-Resources Investigations Report 84-4353, 58 p.

Kernodle, J.M., Miller, R.S., and Scott, W.B., 1987, Three-dimensional model simulation of transient groundwater flow in the Albuquerque-Belen Basin, New Mexico: U.S. Geological Survey Water-Resources Investigations Report 86-4194, 86 p.

Kernodle, J.M., McAda, D.P., and Thorn, C.R., 1995, Simulation of ground-water flow in the Albuquerque Basin, central New Mexico, 1901-1994, with projections to 2020: U.S. Geological Survey Water—Resources Investigations Report 94-4251, 114 p.

Koning, D.J., Pederson, J., Pazzaglia, F.J., and Cather, S.M., 1998, Geology of the Cerro Conejo (Sky Village NE) 7.5-minute quadrangle: New Mexico Bureau of Geology and Mineral Resources, Open-file Geologic Map OF-GM-45, scale 1:24,000.

Koning, D.J., and Personius, S.F., 2002, Geologic map of the Bernalillo NW quadrangle, Sandoval County, New Mexico: U.S. Geological Survey, Miscellaneous Field Studies Map 2404, scale 1:24,000.

Koning, D.J., and Jochems, A.P., 2014, Geologic Map of the Benavidez Ranch 7.5-Minute Quadrangle, Bernalillo and Sandoval Counties, New Mexico: New Mexico Bureau of Geology and Mineral Resources, Open-file Geologic Map 234, scale 1:24,000.

Koning, D.J., and Rawling, G., 2017, Geologic map of the San Felipe Mesa 7.5-minute quadrangle, Sandoval County, New Mexico: New Mexico Bureau of Geology and Mineral Resources, Open-file Geologic Map 266, scale 1:24,000.

Koning, D.J., Heizler, M., and Jochems, A., 2021, Clues from the Santa Fe Group for Oligocene-Miocene paleogeography of the southeastern Colorado Plateau near Grants, NM, *in* Bonnie, F., Kelley, S.A., Zeigler, K.E., McLemore, V.T., Goff, F., and Ulmer-Scholle, D.S., eds., Geology of the Mount Taylor area: New Mexico Geological Society, 71st Annual Fall Field Cofnerence Guidebook, p. 267-280. https://doi.org/10.56577/FFC-71.267

Kozeny, J., 1927, Uber kapillare leitung des wassers im boden: Sitzungsberichte der Akademie der Wissenschaften in Wien, v. 136, p. 271.

Klingbeil, R., Kleineidam, S., Asprion, U., Aigner, T., and Testch, G., 1999, Relating lithofacies to hydrofacies: outcrop-based hydrogeological characterization of Quaternary gravel deposits: Sedimentary Geology, v. 129, p. 299–310.

Lozinsky, R.P., 1988, Stratigraphy, sedimentology, and sand petrology of the Santa Fe Group and pre-Santa Fe Tertiary deposits in the Albuquerque Basin [Ph.D. dissertation]: Socorro, NM, New Mexico Institute of Mining and Technology, 298 p.

Lozinsky, R.P., 1994, Cenozoic stratigraphy, sandstone petrology, and depositional history of the Albuquerque basin, central New Mexico: Geological Society of America, Special Paper 291, p. 73-82.

Machette, M.N., Personius, S.F., Kelson, K.I., Haller, K.M., and Dart, R.L., 1998, Map and data for Quaternary faults and folds in New Mexico: U.S. Geological Survey Open-file report 98-821, 443 p., 1 pl.

Masumura, R., Mikada, H., and Takekawa, J., 2019, The relation between permeability and grain size distribution: The 23rd International Symbosium on Recent Advances in Exploration Geophysics (RAEG 2019), v. 2019, p. 104, https://doi.org/10.3997/2352-8265.20140242

May, J.S., and Russell, L.R., 1994, Thickness of the syn-rift Santa Fe Group in the Albuquerque Basin and its relation to structural style: Geological Society of America, Special Paper 291, p. 113-123.

McAda, D.P., and Barroll, P., 2002, Simulation of ground-water flow in the Middle Rio Grande Basin between Cochiti and San Acacia, New Mexico: U.S. Geological Survey, Water-resources Investigations Report 02-4200, 81 p.

Minor, S.A., and Hudson, M.R., 2006, Regional survey of structural properties and cementation patterns of fault zones in the northern part of the Albuquerque Basin–Implications for ground-water flow: U.S. Geological Survey, Professional Paper 1719, 28 p.

Nelson, P.H., 1994, Permeability-porosity relationships in sedimentary rocks: The Log Analyst, v. 35, no. 3, p. 38-62.

Personius, S.F., 2002, Geologic map of the Santa Ana Pueblo quadrangle, Sandoval County, New Mexico: U.S. Geological Survey, Mescellaneous field Studies Map MF-2405, scale 1:24,000.

Personius, S.F., Machette, M.N., and Stone, B.D., 2000, Preliminary geologic map of the Loma Machette quadrangle, Sandoval County, New Mexico: U.S. Geological Survey, Miscellaneous Field Studies Map MF-2334, scale 1:24,000.

Plummer, L.N., Bexfield, L.M., Anderholm, S.K., Sanford, W. E., and Busenberg, E., 2001, Geochemical characterization of ground-water flow in parts of the Santa Fe Group aquifer system, Middle Rio Grande Basin, New Mexico, in Cole, J.C., ed., U.S. Geological Survey Middle Rio Grande Basin Study—Proceedings of the Fourth Annual Workshop, Albuquerque, New Mexico, February 15-16, 2000: U.S. Geological Survey Open-File Report 00-488, p. 7-10.

1614 Plummer, L.N., Bexfield, L.M., Anderholm, Scott K., Sanford, Ward E., and Busenberg, Eurybiades, 2004a,
1615 Hydrochemical tracers in the Middle Rio Grande Basin, USA: 1. Conceptualization of groundwater
1616 flow. Hydrogeology Journal, v. 12, p. 359-388.

1617 Plummer, L.N., W.E. Sanford, L.M. Bexfield, S.K. Anderholm, and E. Busenberg, 2004b, Using
1618 geochemical data and aquifer simulation to characterize recharge and groundwater flow in the
1619 Middle Rio Grande Basin, New Mexico, *in* Hogan, J.F., Phillips, F.M., and Scanlon, B.R., eds.,
1620 Groundwater Recharge in a Desert Environment: The Southwestern United StatesWater Science and
1621 Applications Series, vol. 9, American Geophysical Union, Washington, D.C., 185-216.

1622 Plummer, L.N., Bexfield, L.M., Anderholm, S.K., Sanford, Ward E., and Busenberg, Eurybiades, 2004c,
1623 Geochemical characterization of ground-water flow in the Santa Fe Group aquifer system, Middle Rio
1624 Grande Basin, New Mexico. U.S. Geological Survey Water-Resources Investigations Report 03-4131
1625 395 p.

1626 Rawling, G.C. and Goodwin, L.B., 2006, Structural record of the mechanical evolution of mixed zones in
1627 faulted poorly lithified sediments, Journal of Structural Geology28: 1623-1639.

1628 Rawling, G.C., Goodwin, L.B., and Wilson, J.L., 2001, Internal architecture, permeability structure, and
1629 hydrologic significance of contrasting fault-zone types: Geology29: 43-46.

1630 Reiter, M., 2001, Using precision temperature logs to estimate horizontal and vertical groundwater flow
1631 components: Water Resources Research, v. 37, no. 3, p. 663-674.

1632 Reiter, M., 2003, Hydrogeothermal studies in the Albuquerque Basin–a geophysical investigation of
1633 ground water flow characteristics: New Mexico Bureau of Geology and Mineral Resources, Circular
1634 211, 74 p.

1635 Riesterer, J., Hawley, J., Drakos, P., Lazarus, J., Lesh, M., and Chudnoff, M. (Glorieta Geoscience, Inc),
1636 2004, City of Rio Rancho Ground water exploration program – Results of Phase One Study;
1637 unpublished consultant report prepared for City of Rio Rancho, Feb. 25, 2004, 112 p.

1638 Riesterer, J., Drakos, P., and Lazarus, J., (Glorieta Geoscience, Inc.), 2008, Evaluation of future production
1639 well locations, well replacement needs, and future water sources, City of Rio Rancho; unpublished
1640 consultant report prepared for City of Rio Rancho by Glorieta Geoscience Inc., Nov. 2008, 18 p.

1641 Riesterer, J., and Drakos, P. (Glorieta Geoscience, Inc.), 2008 (revised 2009), Well drilling, completion,
1642 and testing report, City of Rio Rancho Well 23 (RG-6745-S-27); unpublished consultant report
1643 prepared for City of Rio Rancho by Glorieta Geoscience Inc., August 2008, 45 p. plus an addendum
1644 (14 p.)

1645 Russell, L.R., and Snelson, S., 1994, Structure and tectonic of the Albuquerque Basin segment of the Rio
1646 Grande rift: Insights from reflection seismic data: Geological Society of America, Special Paper 291, p.
1647 83-112.

1648 Sanford Ward E., Plummer L. Niel, McAda, Douglas P., Bexfield, Laura M., Anderholm, Scott K., 2004a,
1649 Hydrochemical tracers in the Middle Rio Grande Basin, USA: 2. Calibration of a groundwater model.
1650 Hydrogeology Journal, v. 12, p. 389-407.

1651 Sanford, W.E., Plummer, L.N., McAda, D.P., Bexfield, L.M., and Anderholm, S.K., 2004b, Use of
1652 environmental tracers to estimate parameters for a predevelopment-ground-water-flow model of
1653 the Middle Rio Grande Basin, New Mexico: U. S. Geological Survey Water-Resources Investigations
1654 Report 03-4286, 102 p.

1655 Smith, G.A., and Lavine, A., 1996, What is the Cochiti Formation?: New Mexico Geological Society,
1656 Guidebook 47, p. 219-224.

1657 Smyth, D.G., 2004, Sedimentology and permeability characteristics of the Arroyo Ojito Formation (Upper
1658 Santa Fe Group) adjacent to the Sand Hill fault, Albuquerque basin, New Mexico [M.S. thesis]:
1659 Socorro, New Mexico Institute of Mining and Technology, 96 p.

1660 Spiegel, Z., 1961, Late Cenozoic sediments of the lower Jemez River region: New Mexico Geological
1661 Society, Guidebook 12, p. 132-138.

1662 Spiegel, Z., and Baldwin, B., 1963, Geology and Water Resources of the Santa Fe Area, New Mexico:
1663 Washington, D.C., Geological Survey Water-Supply Paper 1525, 258 p.

1664 Tedford, R.H., 1982, Neogene stratigraphy of the northwestern Albuquerque basin: New Mexico
1665 Geological Society, Guidebook 33, p. 273-278.

1666 Tedford, R.H., and Barghoorn, S., 1997, Miocene mammals of the Espanola and Albuquerque basins,
1667 north-central New Mexico, *in* Lucas, S.G., Estep, J.W., Williamson, T.E., and Morgan, G.S., eds., New

Mexico's fossil record1: New Mexico Museum of Natural History and Science, Bulletin No. 11, p. 77-95.

Tedford, R.H., and Barghoorn, S., 1999, Santa Fe Group (Neogene), Ceja del Rio Puerco, northwestern Albuquerque Basin, Sandoval County, New Mexico: New Mexico Geological Society, Guidebook 50, p. 327-335.

Tearpock, D.J., and Bischke, R.E., 2002, Applied Subsurface Geological Mapping, with Structural Methods, 2nd edition: Upper Saddle River, New Jersey, Pretince-Hall PTR.

Thompson, R. A., Shroba, R.R., Menges, C.M., Schmidt, D.W., Personius, S.F., and Brandt, T.R., 2009, Geologic map of the Volcanoes Quadrangle, Bernalillo and Sandoval Counties, New Mexico: U.S. Geological Survey, Scientific Investigations Map 3083, scale 1:24,000.

Thorn, C.R., McAda, D.P., and Kernodle, J.M., 1993, Geohydrologic framework and hydrologic conditions in the Albuquerque Basin, central New Mexico: U.S. Geological Survey Water-Resources Investigations Report 93-4149, 106 p.

Urumovic , K., and Urumovic, K., Sr., 2016, The referential grain size and effective porosity in the Kozeny-Carman model: Hdroloogy and Earth System Sciences, v. 20, p. 1669-1680; http://doi.10.5194/hess-20-1669-2016.

Williams, P.L., and Cole, J.C., 2007, Geologic map of the Albuquerque 30' x 60' quadrangle, north-central New Mexico: U.S. Geological Survey, Scientific Investigations Map 2946, 31 p., scale 1:100,000.

Wright, H.E., Jr., 1946, Tertiary and Quaternary geology of the lower Rio Puerco area, New Mexico: Geological Society of America Bulletin, v. 57, p. 383-456.